showed that CD68 did not colocalize with CYGB (Figure 3b–d). LYVE-1, also known as extracellular link domain-containing 1 (XLKD1), acts as a receptor for both soluble and immobilized hyaluronan. Sinusoidal endothelial cells are LYVE-1 positive.[28] We observed LYVE-1 positivity along the hepatic sinusoid in the sinusoidal walls, indicating that

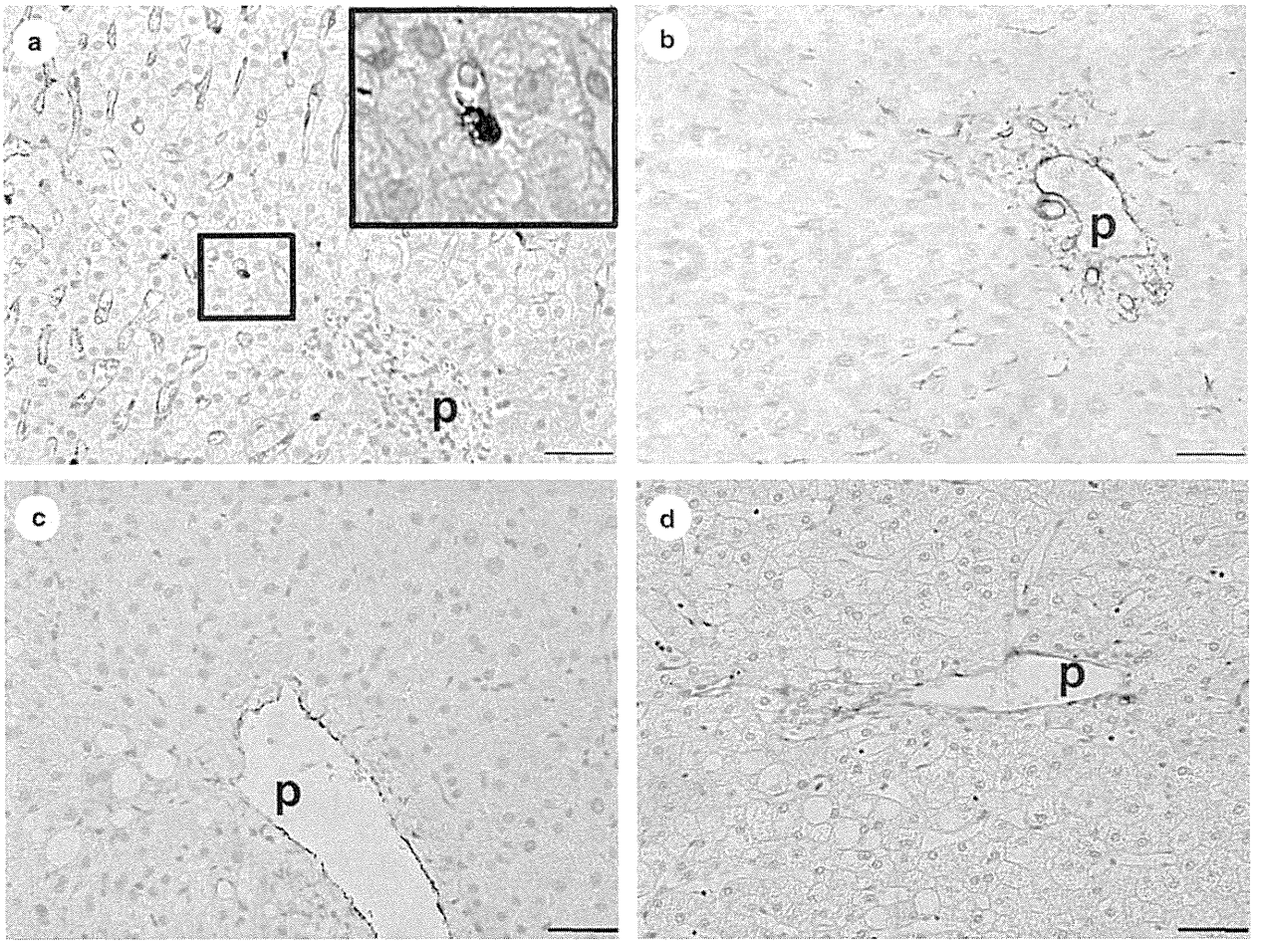

Figure 2 Immunohistochemistry for CRBP-1, α-SMA, FBLN2, and Thy-1 in intact human liver. (**a**) Immunohistochemistry for CRBP-1. In the liver parenchyma, strong expression of CRBP-1 was observed along the sinusoids (arrows). A magnified view of the enclosed area shows that a CRBP-1-positive cell contained lipid droplets, indicating that it was a hepatic stellate cell. CRBP-1 was not observed around the portal area. Bar, 100 μm. p, portal vein. (**b**) Immunohistochemistry for α-SMA. α-SMA-positive cells were present predominantly in the portal area and in the walls of the vessels, but not along the hepatic sinusoids. Bar, 100 μm. (**c**) Immunohistochemistry for FBLN2. FBLN2 was localized in the vessels of the portal spaces. Positive staining for FBLN2 was not visible along the sinusoids. Bar, 100 μm. (**d**) Immunohistochemistry for Thy-1. Thy-1-positive cells were located within the portal tracts adjacent to the wall of the portal vein. Bar, 100 μm.

Figure 1 Characterization of newly generated rabbit polyclonal antibodies against human CYGB. (**a**) Newly generated rabbit polyclonal antibodies against human CYGB detected purified recombinant human CYGB (21 kDa) (lane 1) and EGFP-labeled recombinant human Cygb (48 kDa) (lane 4) but not human albumin (lane 2). LX-2 cells and Huh 7 cells did not express CYGB (lanes 3 and 5, respectively). (1) Recombinant human CYGB (10 μg); (2) human albumin (20 μg); (3) lysate of LX-2 cells (20 μg); (4) lysate of LX-2 cells overexpressing EGFP-CYGB (20 μg); (5) lysate of Huh-7 cells (20 μg). (**b**) Immunohistochemistry of normal human liver tissues. (A) Hematoxylin–eosin staining. No hepatocyte death or inflammation was observed. Bar, 100 μm. c, central vein; p, portal vein. (B) Sirius red staining. Limited collagen deposition was observed around the portal and central vein areas. No fibrosis occurred in the liver parenchyma. Bar, 100 μm. (C) Immunohistochemistry for CYGB using newly generated polyclonal antibodies. CYGB-positive cells were localized in the liver parenchyma along hepatic sinusoids (arrows). Bar, 100 μm. (D) Magnified view of the enclosed area in (C). CYGB-positive cells were present in the perisinusoidal space and contained lipid droplets in the cytoplasm, suggesting that they were stellate cells (arrowheads). Bar, 20 μm. (E) Immunohistochemistry for CYGB using the monoclonal antibody. CYGB-positive cells were localized in the liver parenchyma along the hepatic sinusoids (arrows). Bar, 100 μm. (F) Magnified view of the enclosed area in (E). CYGB-positive cells were present in the perisinusoidal space and contained lipid droplets in the cytoplasm, suggesting that they were stellate cells (arrowheads). Bar, 20 μm.

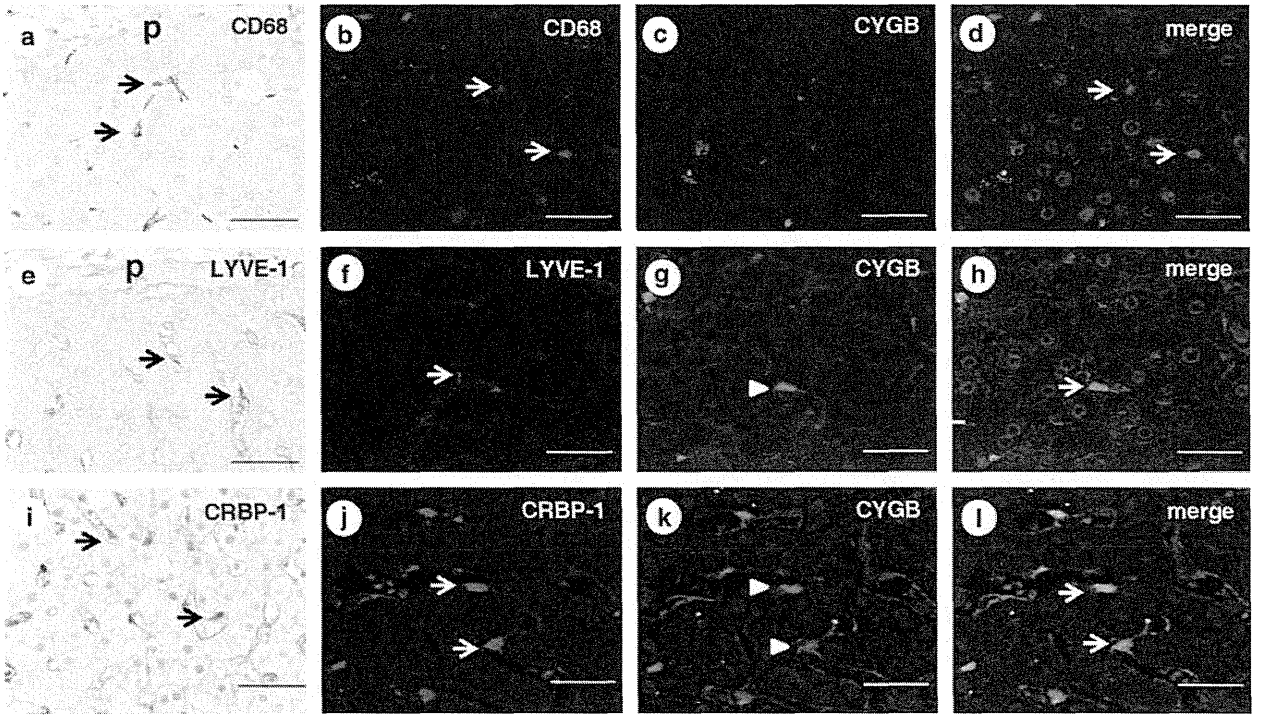

Figure 3 Immunohistochemistry for CD68, LYVE-1, and CRBP-1 in the intact human liver. (**a–d**) Immunohistochemistry for CD68 and CYGB. CD68-positive cells (arrows) were located inside the sinusoidal lumen (**a**). Double immunofluorescence showed that CYGB (**b**) and CD68 (c) did not colocalize as shown in panel **d**. p, portal vein. Bar, 100 μm. (**e–h**) Immunohistochemistry for LYVE-1 and CYGB. LYVE-1-positive cells (arrows) were localized along the hepatic sinusoids (**e**). Double immunofluorescence showed that LYVE-1 (**f**) and CYGB (**g**, arrowhead) did not colocalize, as shown in (**h**). Bar, 100 μm. (**i–l**) Immunohistochemistry for CRBP-1 and CYGB. CRBP-1-positive cells (arrows) were localized in the perisinusoidal space (**i**). Double immunofluorescence showed that CRBP-1 (**j**) and CYGB (**k**, arrowheads) were entirely colocalized, as shown in (**l**). Bar, 100 μm.

LYVE-1-positive cells are sinusoidal endothelial cells in the intact human liver (Figure 3e). Double immunofluorescence staining showed that LYVE-1 did not colocalize with CYGB (Figure 3f–h). Therefore, CYGB was not expressed in hepatocytes, Kupffer cells, or sinusoidal endothelial cells. Double immunostaining for CRBP-1 (Figure 2a and Figure 3i) and CYGB (Figure 3j–l) supported the notion that normal liver tissues contain CYGB- and CRBP-1-double-positive quiescent stellate cells.

CYGB Expression in Fibrotic and Cirrhotic Human Livers

Liver tissues were isolated from patients at different HCV-induced fibrosis stages (from F1 to F4) and subjected to histochemical and immunohistological examination (Figure 4). The extent of collagen deposition at each fibrosis stage was estimated by Sirius red staining, which is shown in Figure 4aA (for F1), E (F2), I (F3), and M (F4). In the liver parenchyma, cells that were positive for CYGB (Figure 4 B, F, J, and N) or CRBP-1 (Figure 4C, G, K, and O) were present along the hepatic sinusoids, indicating that they were stellate cells. α-SMA was expressed in cells around the periportal area, and its expression extended along the expansion of collagen deposition, as shown by Sirius red staining, and along the hepatic sinusoids (Figure 4 D, H, L, and P). Notably, CYGB- and CRBP-1-positive cells (stellate cells) were present inside the hepatic nodules; however, they were scarce in the fibrotic septum of cirrhotic (F4) livers (Figure 4N for CYGB and Figure 4O for CRBP-1), in contrast with the abundance of α-SMA-positive cells in the fibrotic septum (Figure 4P). We further studied the expression of CYGB, CRBP-1, and α-SMA in human NASH tissue (fibrosis stage F2). The results were similar to those obtained in HCV-induced fibrotic tissue: CYGB- and CRBP-1-positive cells were present along the hepatic sinusoids in the liver parenchyma, and α-SMA was expressed by cells around the portal area, with its expression extending along the deposited collagen (Figure 4Q, R, and S).

To quantify the immunohistochemistry results, we performed immunoblot analysis using rabbit polyclonal anti-human CYGB antibodies, which specifically react with human CYGB but not mouse CYGB, in human liver samples and fibrotic mouse livers. We detected a band at the position of purified recombinant human CYGB (21 kDa) in HCV-infected human fibrotic liver tissues at the F2 stage; however, this band was not detected in normal human liver samples. In addition, no CYGB band was observed in fibrotic liver tissues from mice treated with a choline-deficient amino acid-defined diet (for 32 weeks) or *N*,*N*-diethylnitrosamine

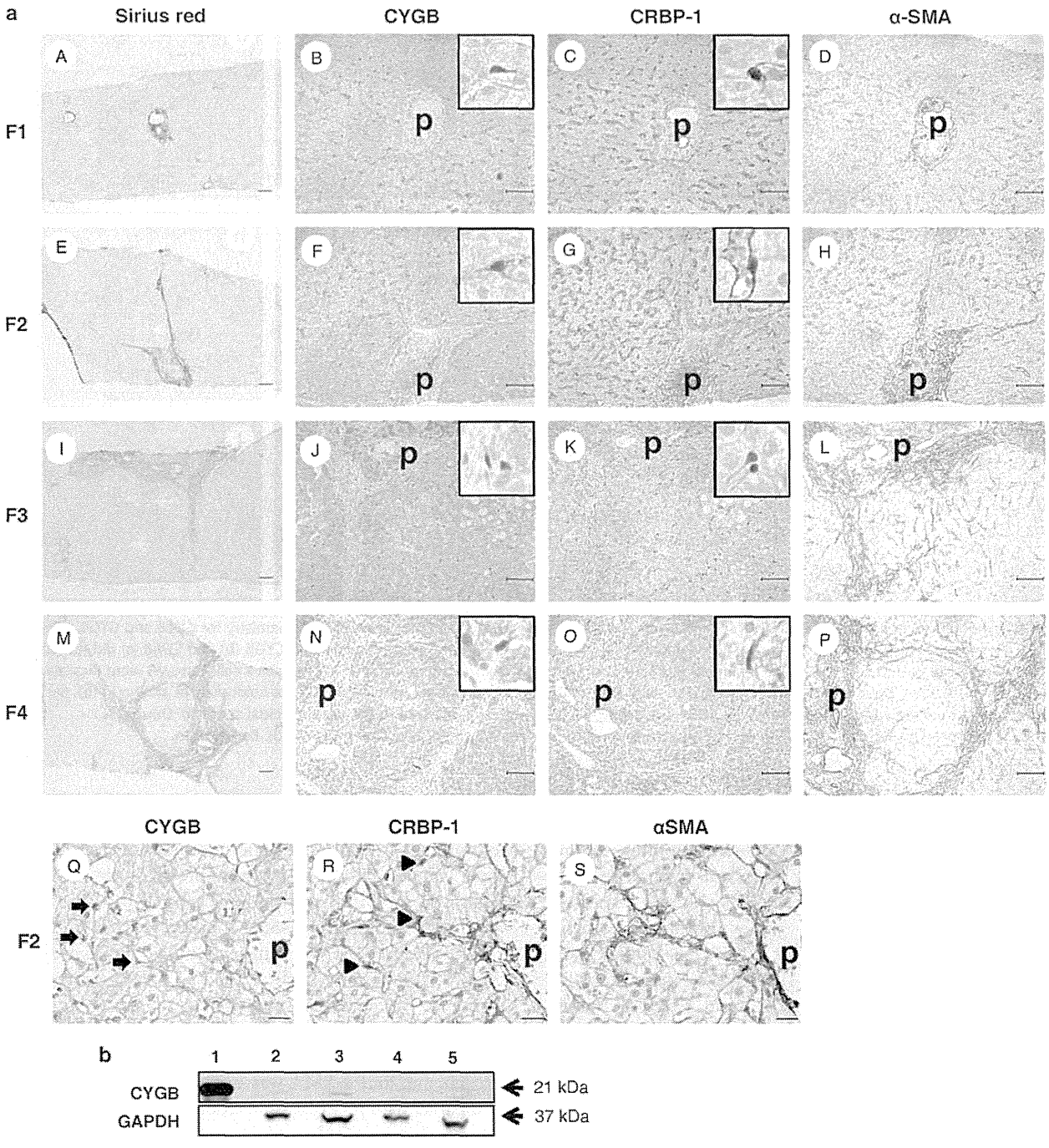

Figure 4 (**a**) Histological analyses of human liver fibrosis at different stages (F1 to F4) according to the new Inuyama classification. (A, E, I, M) Sirius red staining. Bar, 50 μm. (B, F, J, N, Q) Immunohistochemistry for CYGB. Bar, 50 μm. Inserts show high-magnification views of CYGB-positive cells in the liver parenchyma. (C, G, K, O, R) Immunohistochemistry for CRBP-1. Bar, 50 μm. Inserts show high-magnification views of CRBP-1-positive cells in the liver parenchyma. (D, H, L, P, S) Immunohistochemistry for α-SMA. Bar, 50 μm. p, portal vein. (**b**) Immunoblot analysis using rabbit polyclonal anti-human CYGB antibodies that specifically react with human CYGB but not mouse CYGB, with human liver samples and fibrotic mouse livers. (1) Recombinant human CYGB (10 μg); (2) normal human liver (25 μg); (3) hepatitis C virus-infected human liver (25 μg); (4) fibrotic liver from a mouse treated with a choline-deficient amino acid-defined diet (25 μg); and (5) fibrotic liver from a mouse treated with *N,N*-diethylnitrosamine (25 μg). Note that this analysis also revealed the induction of CYGB in fibrotic human livers.

(25 p.p.m. for 25 weeks). Thus, this analysis also revealed the induction of CYGB in fibrotic human livers (Figure 4b).

The scarcity of CYGB- and CRBP-1-positive cells in the fibrotic septum is convincingly shown in Figure 5. The distribution patterns of three myofibroblast biomarkers, α-SMA (Figure 5b, e, h, k, n), Thy-1 (Figure 5c, f, i, and l), and FBLN2 (Figure 5o), in the portal areas were nearly identical in fibrotic livers. The distribution of CYGB was mutually exclusive with the distribution of these three proteins (Figure 5a, d, g, j, and m).

The mutually exclusive localization patterns of these cell type-specific markers were further examined by double immunofluorescence staining (Figure 6). CYGB was expressed in cells close to the parenchymal area of F1 to F3 livers (Figure 6a, d, and g), and its expression did not overlap with that of α-SMA (Figure 6c, f, and i). However, in the F4 liver, cells near the extended fibrotic septum were double positive for CYGB and α-SMA, strongly suggesting that these cells were activated stellate cells. In the F3 liver, neither FBLN2 nor Thy-1 overlapped with CYGB (Figure 6m–r).

Taken together, these data reveal that CYGB and CRBP-1 are excellent markers of human stellate cells in both intact and fibrotic livers and that stellate cells become positive for α-SMA when activated. We hypothesize that cells positive for FBLN2 and Thy-1 are different from stellate cells and exhibit the phenotype of portal myofibroblasts that are α-SMA positive in intact human liver tissue.

Quantitative Analysis of the Contributions of Stellate Cells and Myofibroblasts to the Progression of Fibrosis

Of the 40 HCV-infected patients who underwent liver biopsy, the proportion of fibrotic area (as determined by Sirius red staining and immunostaining for α-SMA and Thy-1) was significantly correlated with the stage of liver fibrosis according to the new Inuyama classification. The Sirius red-positive area increased from 1.8% in F1 to 3.66%, 8.57%, and 16.8% in F2, F3, and F4, respectively (Figure 7a). Similarly, the α-SMA-positive area increased from 1.26% in F1 to 1.82%, 5.65%, and 8.31% in F2, F3, and F4, respectively (Figure 7b). The Thy-1-positive area increased from 1.13% in F1 to 2.13%, 5.43%, and 7.52% in F2, F3, and F4, respectively (Figure 7c). In contrast, the density of CYGB-positive cells (Figure 7d) and CRBP-1-positive cells (Figure 7e) was inversely correlated with the progression of liver fibrosis; the density of CYGB-positive cells was 17.9 ± 1.29, 19.7 ± 1.01, 16.2 ± 0.82, and 13.8 ± 1.06 cells/mm^2 in F1, F2, F3, and F4, respectively, and the density of CRBP-1-positive cells was 9.56 ± 1.24, 14.6 ± 0.77, 12.1 ± 0.83, and 9 ± 0.67 cells/mm^2 in F1, F2, F3, and F4, respectively.

CYGB Expression in Primary Mouse Stellate Cells

We determined above the *in vivo* expression profiles of cell type-specific biomarkers in stellate cells and myofibroblasts in intact and fibrotic human liver tissues. Next, we questioned whether these *in vivo* expression profiles could be reproduced in an *in vitro* system. We utilized primary cultures of mouse stellate cells rather than human stellate cells because human stellate cells in a normal quiescent stage are difficult to obtain for laboratory use. These cells were cultured for up to 7 days, during which changes in the expression levels of CYGB, α-SMA, and Thy-1 were immunohistochemically examined (Figure 8).

At 1 day of culture after isolation from the intact liver, mouse stellate cells adhered to plastic plates and exhibited round cell bodies with numerous lipid droplets similar to those observed in lipocytes (Figure 8aA). The cell bodies then began to gradually spread and flatten, and they successively increased in size and lost their lipid droplets, resulting in an activated myofibroblastic phenotype (Figure 8aB and C). Immunocytochemical analyses confirmed the consistent expression of CYGB until day 7 of culture (Figure 8aA–C). α-SMA was not observed at day 1 (Figure 8aD); however, it later appeared at days 4 and 7 (Figure 8aE and F). Double immunofluorescence analysis confirmed the presence of both CYGB and α-SMA in stellate cells at days 4 and 7 (Figure 8aH and J), although their intracellular localization patterns were different; Cygb was distributed diffusely in the cytoplasm, whereas α-SMA tended to accumulate at the periphery of the cells. Immunostaining for CRBP-1 and α-SMA yielded similar results, although CRBP-1 expression was decreased in 7-day-cultured stellate cells, presumably because of the loss of vitamin A in the cytoplasm (data not shown). Thy-1 was not observed throughout the culture period (Figure 8aM–O). The above-mentioned expression profiles of the marker proteins were confirmed by immunoblot analysis (Figure 8b). These results led us to hypothesize that the α-SMA-positive cells observed at later stages of culture were not myofibroblasts but rather activated stellate cells because they were Thy-1 negative.

DISCUSSION

Cytoglobin Is an Excellent Marker of Human Stellate Cells

CYGB was previously isolated from cultured rat hepatic stellate cells that have vitamin A storage ability in the quiescent state and function as liver-specific pericytes.[1]

Figure 5 Histological analyses of human liver fibrosis at different stages (F1 to F4) according to the new Inuyama classification. Immunohistochemistry for CYGB (**a**, **d**, **g**, **j**, **m**), α-SMA (**b**, **e**, **h**, **k**, **n**), Thy-1 (**c**, **f**, **i**, **l**), and FBLN2 (**o**). At each stage, CYGB (arrows) had limited expression in sinusoids, and the positive cells were deemed stellate cells. α-SMA was expressed in the vessel walls of the portal vein and artery, around bile ducts, and in the cells in Glisson's capsule. Some α-SMA-positive cells were also present in the parenchyma at stage F4 (**k**). Both Thy-1 and FBLN2 had limited expression in Glisson's capsule and the extended fibrotic septum in all stages of liver fibrosis. Bar, 50 μm. p, portal vein.

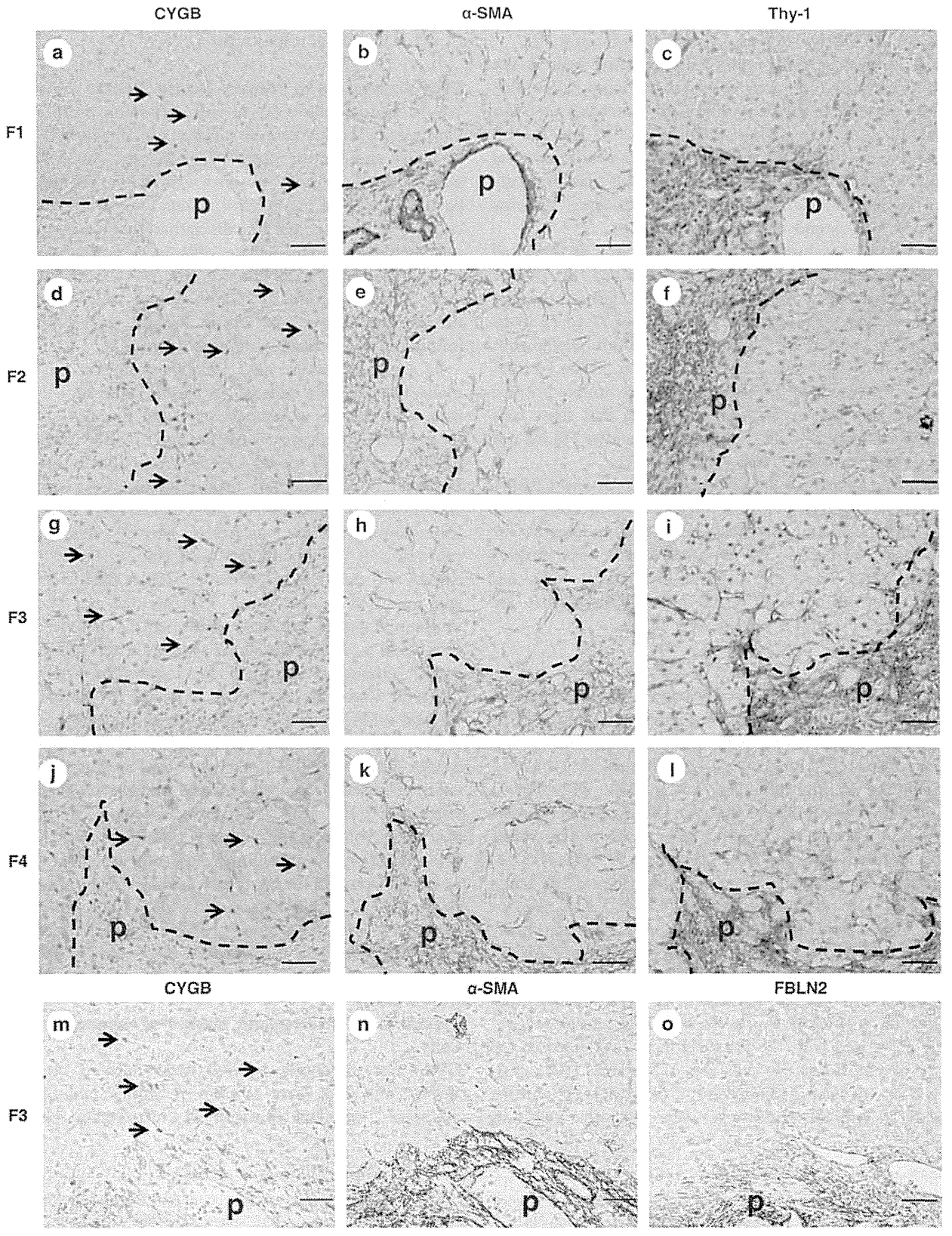
CYGB
α-SMA
Thy-1
F1
F2
F3
F4
CYGB
α-SMA
FBLN2
F3
a
b
c
d
e
f
g
h
i
j
k
l
m
n
o
p

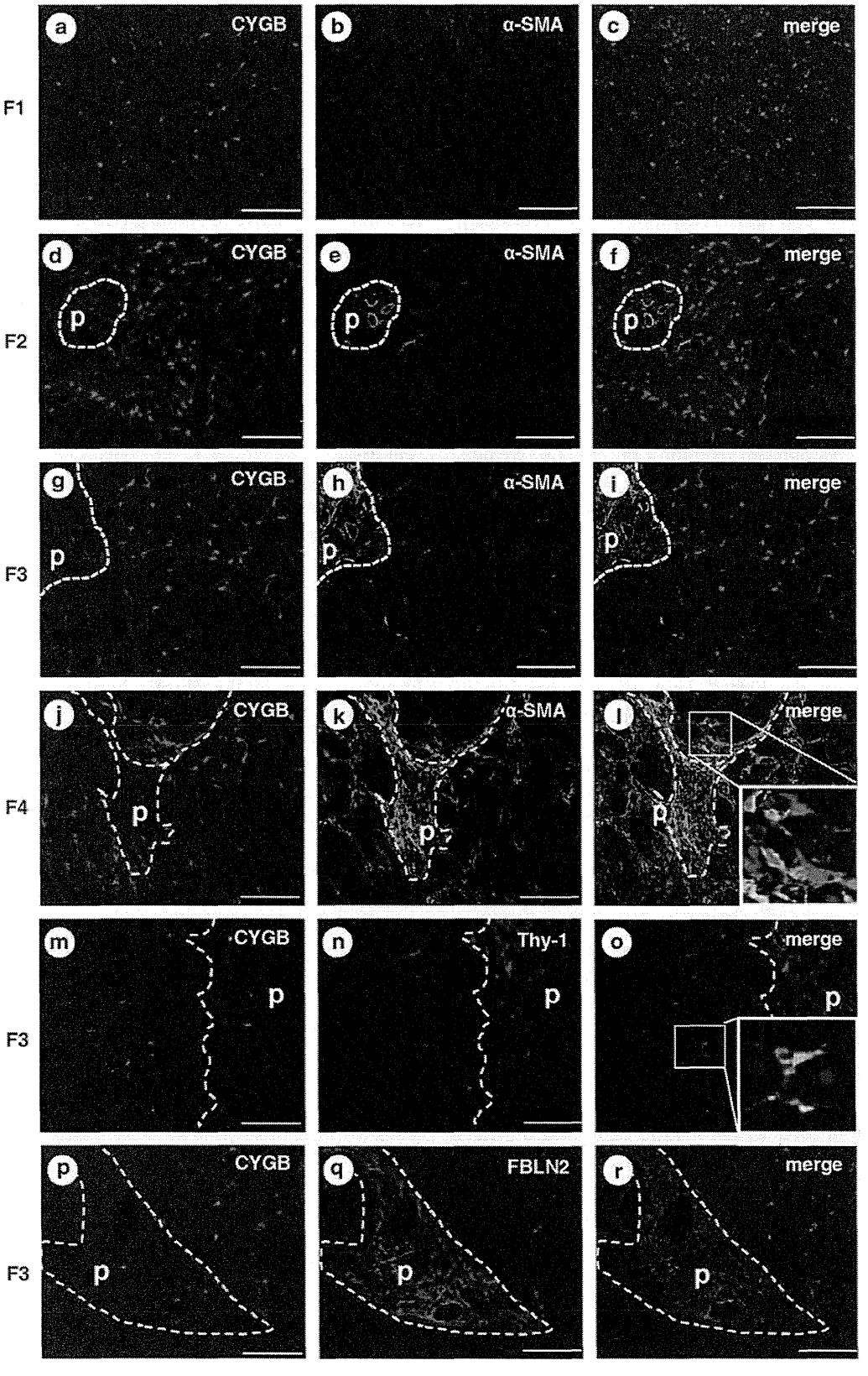
F1
a
CYGB
b
α-SMA
c
merge
F2
d
CYGB
p
e
α-SMA
p
f
merge
p
F3
g
CYGB
p
h
α-SMA
p
i
merge
p
F4
j
CYGB
p
k
α-SMA
p
l
merge
p
F3
m
CYGB
p
n
Thy-1
p
o
merge
p
F3
p
CYGB
p
q
FBLN2
p
r
merge
p

Histoglobin, CYGB, and stellate cell activation-associated protein were classified as human, mouse, and rat homologs of a hexacoordinate globin that differs from the traditional pentacoordinate globins such as myoglobin and hemoglobin.[1–4] CYGB is induced during the activation of rat hepatic stellate cells, which become myofibroblast-like cells, and its expression is increased in fibrotic livers in rodent models.[1] However, it is unclear whether CYGB is expressed in both stellate cells and portal myofibroblasts. Previously, Ogawa *et al*[21] isolated vitamin A-free cells from the nonparenchymal cell fraction in rat livers using FACS analysis. Ogawa *et al*[21] then demonstrated that vitamin A-positive cells are desmin, CYGB, and α-SMA positive and also highly express oxidized low-density lipoprotein receptor 1, endothelin receptor B, and cardiac troponin T. In contrast, vitamin A-free cells are negative for desmin and CYGB but positive for α-SMA and FBLN2. These cell types express high levels of arginine vasopressin receptor V1a (Avpr1a), gremlin, osteopontin, collagen a3(V), and lumican. Thus, Ogawa *et al*[21] concluded that CYGB could be a promising molecular marker of rat hepatic stellate cells. Furthermore, Bosselut *et al*[29] performed a comparative proteomic study to identify markers and gain insight into the distinct functions of myofibroblasts derived from either hepatic stellate cells or portal mesenchymal cells in rats.[21] The two cell types were subjected to comparative analyses by 2-D MS/MS. CYGB was confirmed to have the highest level of overexpression in activated stellate cells, as confirmed by reverse-transcription quantitative real-time PCR, immunoblot, and immunocytochemical analyses. Thus, CYGB was identified as the best marker for distinguishing stellate cells from portal myofibroblasts. The results also suggested different functions for the two cell populations in the liver wound-healing response, with a prominent role for portal myofibroblasts in scar formation. It should be noted that these previous studies confirmed the expression of CYGB in rodent hepatic stellate cells and *in vivo* models, whereas the present study addressed the actual localization of CYGB in human stellate cells, but not in portal myofibroblasts that are positive for FBLN2 and Thy-1.

Definition of Hepatic Myofibroblasts

The term 'myofibroblast' was first proposed by Gabbiani *et al*[30] in 1972 to refer to fibroblastic cells located within granulation tissue that exhibit substantial cytoplasmic microfilaments composed of actin, myosin, and associated proteins.[29] In particular, the microfilaments of myofibroblasts contain α-SMA that is the actin isoform typical of smooth muscle cells located in the vessel wall[30] and has become the most reliable marker for myofibroblastic cells.[31,32] Myofibroblasts are additionally positive for Thy-1.[12,13]

In the liver, hepatic stellate cells and portal fibroblasts are able to acquire a myofibroblastic phenotype,[8,33] although it has remained difficult to distinguish myofibroblastic (activated) stellate cells from portal myofibroblasts in human liver tissue. In the current study, we showed that cells that are positive for both CYGB and CRBP-1 represent the quiescent phenotype of human stellate cells that are uniquely localized in the perisinusoidal space, and cells that are additionally positive for α-SMA are myofibroblastic (activated) human stellate cells that are predominantly present near the fibrotic septum of advanced fibrotic liver tissues. Furthermore, we observed that cells positive for Thy-1 and FBLN2 in normal liver tissues (ie, portal myofibroblasts) were present but scarce around the portal vein area.

Dudas *et al*[12] first reported that Thy-1 is an *in vivo* and *in vitro* marker of rat hepatic myofibroblasts, and later confirmed that Thy-1 is not present in normal or capillarized sinusoids or in isolated rat stellate cells, and that it is neither inducible in isolated stellate cells nor upregulated in myofibroblasts.[14] In accordance with this report, we detected Thy-1 positivity to a limited extent around the portal vein area in the intact human liver and in the extended fibrotic septum of the fibrotic human liver, where portal myofibroblasts are located. Culture experiments using mouse stellate cells confirmed that these cells express CYGB throughout the culture period until day 7 and α-SMA at days 4 and 7, whereas Thy-1 is not expressed throughout this period. Thus, our data also support the hypothesis that Thy-1 is not a marker of hepatic stellate cells in humans or mice, although it is expressed in myofibroblasts around the portal vein area. The reason for the minimal expression of Thy-1 in portal myofibroblasts is not known, although Thy-1 regulates fibroblast focal adhesions, cytoskeletal organization, and cell migration.[34]

FBLN2 is an extracellular matrix protein of the fibulin family that binds various extracellular ligands and calcium. FBLN2 is present in the basement membrane and stroma of several tissues and may play a role in organ development, particularly during the differentiation of heart, skeletal, and neuronal structures. Knittel *et al*[15] reported that FBLN2-positive MFs are detectable in the portal field, vessel walls, and hepatic parenchyma of the normal liver, and their number is increased in the septal regions during liver fibrogenesis in rat models. These findings are similar to

Figure 6 Double immunofluorescence staining. CYGB (red in panels **a**, **d**, **g**, and **j**; green in panels **m** and **p**), α-SMA (green in panels **b**, **e**, **h**, and **k**), DAPI (blue), Thy-1 (red in panel **n**), and FBLN2 (red in panel **q**) are shown. Merged photographs of CYGB and α-SMA, FBLN2, or Thy-1 are also presented. CYGB was expressed in the parenchyma and inside hepatocytic nodules. Cells constituting the fibrotic septum in advanced fibrosis (F3) were positive for α-SMA but negative for CYGB. CYGB and α-SMA double-positive cells were occasionally present around the fibrotic septum of F4 liver (**i**). CYGB-positive cells did not overlap with cells that were positive for Thy-1 or FBLN2 (**o** and **r**). Bar, 100 μm.

our present observations in diseased human livers. Thus, FBLN2 and Thy-1 are reliable cellular markers of portal myofibroblasts that differ from stellate cells that are positive for CYGB and CRBP-1 in intact and fibrotic human livers. In the portal area, MFs that are negative for CYGB are the main cells that induce fibrotic septum formation. Thus, targeting of these cells in addition to stellate cells has therapeutic potential for controlling fibrotic septum development.

Cellular Markers of Hepatic Stellate Cells

Based on our present results, we emphasize the superiority of CYGB as a marker of human stellate cells in both intact and fibrotic livers. Several markers of stellate cells have been reported in rodents and humans. Stellate cells store vitamin A-containing lipid droplets, suggesting that vitamin A may be a useful marker of stellate cells.[35] However, a specific staining method to identify vitamin A or related compounds,

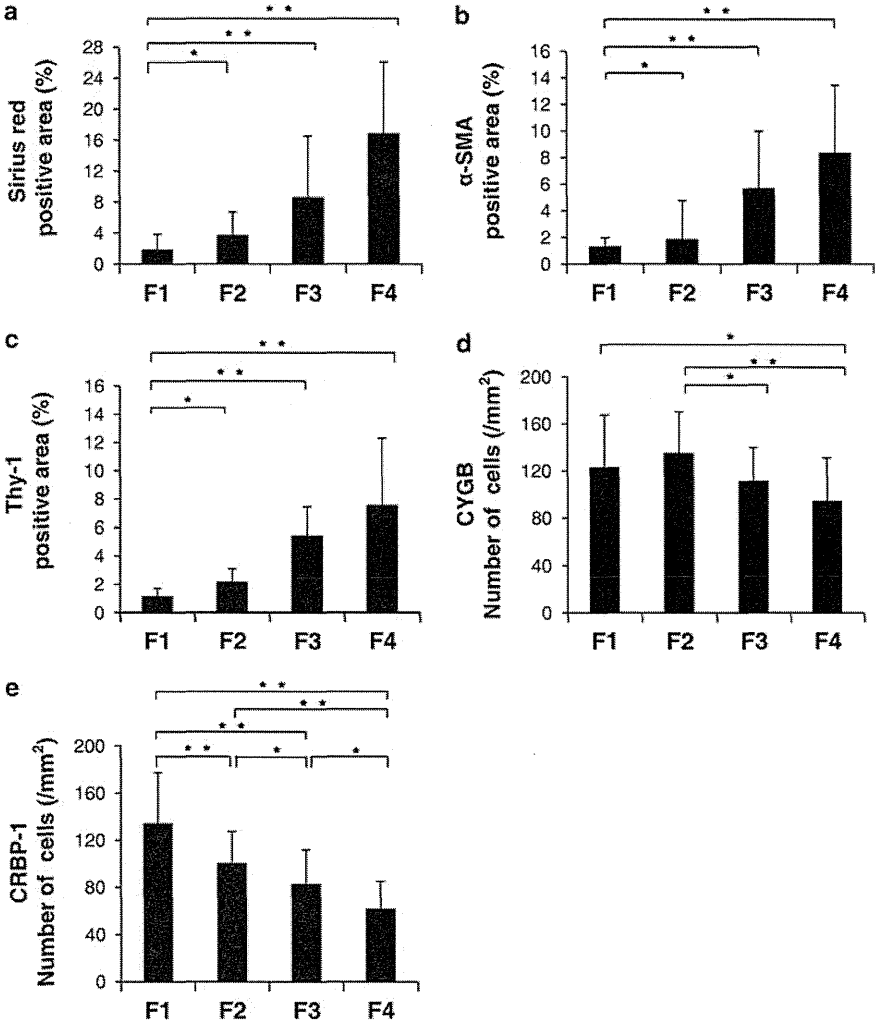

Figure 7 Morphometric analysis. (**a–c**) Correlation between hepatic fibrosis stage (according to the new Inuyama classification) and the ratio of the Sirius red-positive area (**a**), α-SMA-positive area, (**b**) or Thy-1-positive area (**c**). Positive areas for Sirius red, α-SMA, or Thy-1 immunohistochemistry were determined using Lumina Vision 2.4 bio-imaging software (Mitani Corporation, Tokyo, Japan). Note that the Sirius red-positive area, α-SMA-positive area, and Thy-1-positive area increased with the progression of liver fibrosis. (**d**, **e**) CYGB or CRBP-1-positive cells were counted in a 1.4 mm^2 area under a × 100 objective. Note that the CYGB- and CRBP-1-positive cell numbers decreased as liver fibrosis progressed. $^*P<0.05$, $^{**}P<0.01$.

Figure 8 CYGB expression in primary cultured mouse stellate cells. After 1 day of culture following isolation, mouse HSCs adhered to plastic plates and exhibited round cell bodies with numerous lipid droplets similar to those observed in lipocytes. Cell bodies then began to gradually spread and flatten, increasing in size and losing lipid droplets, resulting in the activated myofibroblastic phenotype. (**a**) Immunocytochemical analyses confirmed the expression of CYGB throughout the experimental period (A–C), and α-SMA was detected at days 4 and 7 (D–F). Double immunofluorescence showed that activated mouse stellate cells were positive for both Cygb and α-SMA (G, H, I). Under identical culture conditions, Thy-1 was not observed in mouse stellate cells (M, N, O) that were positive for Cygb (J–L, P–R). Bar, 20 μm. (**b**) Immunoblot analyses confirmed the presence of CYGB at days 1, 4, and 7 and α-SMA at days 4 and 7. Thy-1 was not detected throughout the culture period.

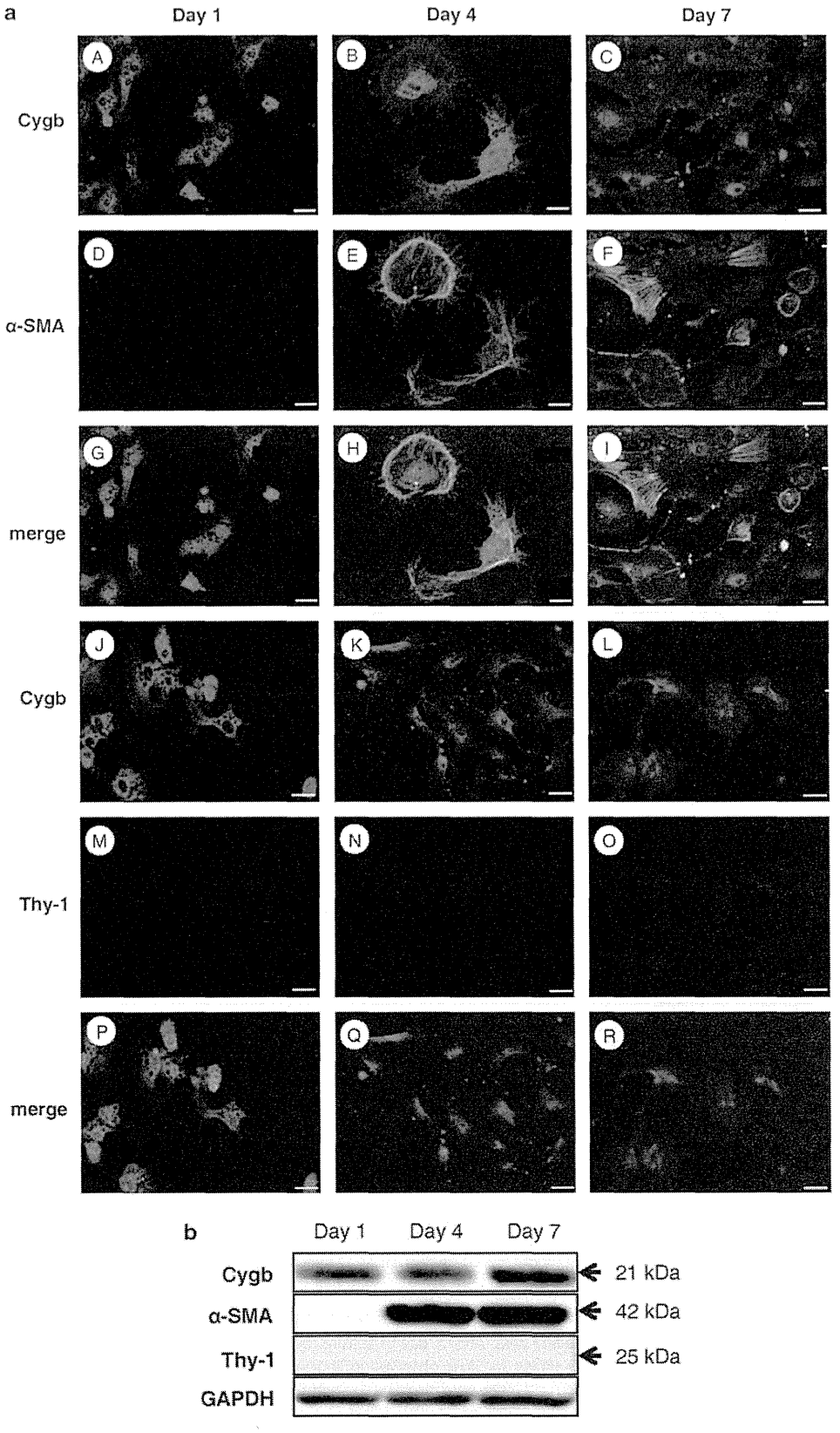
a
Day 1
Day 4
Day 7
Cygb
α-SMA
merge
Cygb
Thy-1
merge
A
B
C
D
E
F
G
H
I
J
K
L
M
N
O
P
Q
R
b
Day 1
Day 4
Day 7
Cygb
α-SMA
Thy-1
GAPDH
21 kDa
42 kDa
25 kDa

such as retinol and retinoic acid, has not been developed, and detection of these compounds via fluorescence microscopy is inconvenient for fixed human liver tissues obtained via clinical procedures. In this context, the use of CRBP-1, a carrier protein of intracellular retinol, is reasonable.[11] CRBP-1 was observed to be downregulated in human livers with advanced fibrosis (Figure 7), presumably because of the loss of vitamin A in stellate cells upon cell activation.

As discussed above, α-SMA is frequently used as a marker of activated and myofibroblastic stellate cells.[29–33] However, this cytoskeletal protein is also expressed in portal myofibroblasts and vascular smooth muscle cells in the arteries, portal vein, and central veins, indicating that α-SMA is not specific for stellate cells. Vinculin, a membrane-cytoskeletal protein in focal adhesion plaques, and synemin, an intermediate filament, show localization patterns similar to that of α-SMA.[36,37]

Desmin, a 52 kD protein that is a subunit of intermediate filaments in skeletal muscle, smooth muscle, and cardiac muscle, was originally identified as a stellate cell marker by Yokoi *et al*[10] in 1984. Desmin is clearly detectable in mouse and rat stellate cells in tissue and in primary culture but not expressed by human stellate cells. Furthermore, desmin expression in rodent hepatic stellate cells has been reported to be both heterogeneous and location dependent.[38] Thus, desmin is no longer considered to be a specific marker of stellate cells. Although neural cell adhesion molecule (also known as CD56) and the intermediate proteins glial fibrillary acidic protein and vimentin have frequently been used as markers of stellate cells, these proteins are also expressed by myofibroblasts.[39,40] In addition, although neurotrophin-3 is specific for stellate cells, it disappears in activated stellate cells in human tissue.[41]

CONCLUSIONS

Taken together, our findings reveal that CYGB is an excellent marker for quiescent and activated stellate cells in both intact and fibrotic human liver. Because the identity of the cell types that participate in collagen production and the fibrotic process in the diseased human liver (caused by hepatitis B or C virus infection, alcohol abuse, obesity, or autoimmune disease) is controversial and because myofibroblasts can be derived from stellate cells, portal myofibroblasts, mesothelial cells,[42] and the epithelial–mesenchymal transition,[43] a molecular marker that is able to uniquely trace stellate cells inhuman liver tissues will be valuable for studying the pathogenesis and fibrotic process of human liver disease.

ACKNOWLEDGMENTS

We thank Professor Kazuo Ikeda and Dr Keiko Iwaisako, Osaka City University Medical School, for their valuable comments on this study. This work was supported by a Grant-in-Aid for Scientific Research from the Japan Society for the Promotion of Science (JSPS) (no. 21390232; 2009–2011; to NK); a grant from the Ministry of Health, Labour, and Welfare of Japan (2008–2010; to NK); and a Thrust Area Research Grant from Osaka City University (2008–2012; to NK).

DISCLOSURE/CONFLICT OF INTEREST

The authors declare no conflict of interest.

1. Kawada N, Kristensen DB, Asahina K, *et al.* Characterization of a stellate cell activation-associated protein (STAP) with peroxidase activity found in rat hepatic stellate cells. J Biol Chem 2001;276:25318–25323.
2. Trent 3rd JT, Hargrove MS. A ubiquitously expressed human hexacoordinate hemoglobin. J Biol Chem 2002;277:19538–19545.
3. Burmester T, Ebner B, Weich B, *et al.* Cytoglobin: a novel globin type ubiquitously expressed in vertebrate tissues. Mol Biol Evol 2002;19:416–421.
4. Pesce A, Bolognesi M, Bocedi A, *et al.* Neuroglobin and cytoglobin. Fresh blood for the vertebrate globin family. EMBO Rep 2002;3:1146–1151.
5. Sawai H, Kawada N, Yoshizato K, *et al.* Characterization of the heme environmental structure of cytoglobin, a fourth globin in humans. Biochemistry 2003;42:5133–5142.
6. Schmidt M, Gerlach F, Avivi A, *et al.* Cytoglobin is a respiratory protein in connective tissue and neurons, which is up-regulated by hypoxia. J Biol Chem 2004;279:8063–8069.
7. Geuens E, Brouns I, Flamez D, *et al.* A globin in the nucleus! J Biol Chem 2003;278:30417–30420.
8. Friedman SL. Hepatic stellate cells: protean, multifunctional, and enigmatic cells of the liver. Physiol Rev. 2008;88:125–172.
9. Scholten D, Osterreicher CH, Scholten A, *et al.* Genetic labeling does not detect epithelial-to-mesenchymal transition of cholangiocytes in liver fibrosis in mice. Gastroenterology 2010;139:987–998.
10. Yokoi Y, Namihisa T, Kuroda H, *et al.* Immunocytochemical detection of desmin in fat-storing cells (Ito cells). Hepatology 1984;4:709–714.
11. Uchio K, Tuchweber B, Manabe N, *et al.* Cellular retinol-binding protein-1 expression and modulation during in vivo and in vitro myofibroblastic differentiation of rat hepatic stellate cells and portal fibroblasts. Lab Invest 2002;82:619–628.
12. Dudas J, Mansuroglu T, Batusic D, *et al.* Thy-1 is an in vivo and in vitro marker of liver myofibroblasts. Cell Tissue Res 2007;329:503–514.
13. Dezso K, Jelnes P, László V, *et al.* Thy-1 is expressed in hepatic myofibroblasts and not oval cells in stem cell-mediated liver regeneration. Am J Pathol 2007;171:1529–1537.
14. Dudas J, Mansuroglu T, Batusic D, *et al.* Thy-1 is expressed in myofibroblasts but not found in hepatic stellate cells following liver injury. Histochem Cell Biol 2009;131:115–127.
15. Knittel T, Kobold D, Saile B, *et al.* Rat liver myofibroblasts and hepatic stellate cells: different cell populations of the fibroblast lineage with fibrogenic potential. Gastroenterology 1999;117:1205–1221.
16. Uyama N, Iimuro Y, Kawada N, *et al.* Fascin, a novel marker of human hepatic stellate cells, may regulate their proliferation, migration, and collagen gene expression through the FAK-PI3K-Akt pathway. Lab Invest 2012;92:57–71.
17. Piscaglia F, Dudás J, Knittel T, *et al.* Expression of ECM proteins fibulin-1 and -2 in acute and chronic liver disease and in cultured rat liver cells. Cell Tissue Res 2009;337:449–462.
18. Janiec DJ, Jacobson ER, Freeth A, *et al.* Histologic variation of grade and stage of non-alcoholic fatty liver disease in liver biopsies. Obes Surg 2005;15:497–501.
19. Ichida F, Tsuji T, Omata M, *et al.* New Inuyama classification; new criteria for histological assessment of chronic hepatitis. Int Hepatol Com 1996;6:112–119.
20. Mori M, Fujii H, Ogawa T, *et al.* Close correlation of liver stiffness with collagen deposition and presence of myofibroblasts in non-alcoholic fatty liver disease. Hepatol Res 2011;41:897–903.
21. Ogawa T, Tateno C, Asahina K, *et al.* Identification of vitamin A-free cells in a stellate cell-enriched fraction of normal rat liver as myofibroblasts. Histochem Cell Biol 2007;127:161–174.
22. Xu L, Hui AY, Albanis E, *et al.* Human hepatic stellate cell lines, LX-1 and LX-2: new tools for analysis of hepatic fibrosis. Gut 2005;54:142–151.
23. Kristensen DB, Kawada N, Imamura K, *et al.* Proteome analysis of rat hepatic stellate cells. Hepatology 2000;32:268–277.
24. Mu YP, Ogawa T, Kawada N. Reversibility of fibrosis, inflammation, and endoplasmic reticulum stress in the liver of rats fed a methionine-choline-deficient diet. Lab Invest 2010;90:245–256.

25. Nakatani K, Okuyama H, Shimahara Y, *et al.* Cytoglobin/STAP, its unique localization in splanchnic fibroblast-like cells and function in organ fibrogenesis. Lab Invest 2004;84:91–101.
26. Sugimoto H, Makino M, Sawai H, *et al.* Structural basis of human cytoglobin for ligand binding. J Mol Biol 2004;339:873–885.
27. Mathew J, Hines JE, Toole K, *et al.* Quantitative analysis of macrophages and perisinusoidal cells in primary biliary cirrhosis. Histopathology 1994;25:65–70.
28. Mouta Carreira C, Nasser SM, di Tomaso E, *et al.* LYVE-1 is not restricted to the lymph vessels: expression in normal liver blood sinusoids and down-regulation in human liver cancer and cirrhosis. Cancer Res 2001;61:8079–8084.
29. Bosselut N, Housset C, Marcelo P, *et al.* Distinct proteomic features of two fibrogenic liver cell populations: hepatic stellate cells and portal myofibroblasts. Proteomics 2010;10:1017–1028.
30. Gabbiani G, Majno G. Dupuytren's contracture: fibroblast contraction? An ultrastructural study. Am J Pathol 1972;66:131–146.
31. Darby I, Skalli O, Gabbiani G. Alpha-smooth muscle actin is transiently expressed by myofibroblasts during experimental wound healing. Lab Invest 1990;63:21–29.
32. Gabbiani G. The myofibroblast in wound healing and fibrocontractive diseases. J Pathol 2003;200:500–503.
33. Desmoulière A, Tuchweber B, Gabbiani G. Role of the myofibroblast differentiation during liver fibrosis. J Hepatol 1995;22(2 Suppl):61–64.
34. Niki T, Rombouts K, De Bleser P, *et al.* A histone deacetylase inhibitor, trichostatin A, suppresses myofibroblastic differentiation of rat hepatic stellate cells in primary culture. Hepatology 1999;29:858–867.
35. Wake K. Perisinusoidal stellate cells (fat-storing cells, interstitial cells, lipocytes), their related structure in and around the liver sinusoids, and vitamin A-storing cells in extrahepatic organs. Int Rev Cytol 1980;66:303–353.
36. Rege TA, Hagood JS. Thy-1 as a regulator of cell-cell and cell-matrix interactions in axon regeneration, apoptosis, adhesion, migration, cancer, and fibrosis. FASEB J 2006;20:1045–1054.
37. Kawai S, Enzan H, Hayashi Y, *et al.* Vinculin: a novel marker for quiescent and activated hepatic stellate cells in human and rat livers. Virchows Arch 2003;443:78–86.
38. Uyama N, Zhao L, Van Rossen E, *et al.* Hepatic stellate cells express synemin, a protein bridging intermediate filaments to focal adhesions. Gut 2006;55:1276–1289.
39. Wake K, Sato T. Intralobular heterogeneity of perisinusoidal stellate cells in porcine liver. Cell Tissue Res 1993;273:227–237.
40. Nakatani K, Seki S, Kawada N, *et al.* Expression of neural cell adhesion molecule (N-CAM) in perisinusoidal stellate cells of the human liver. Cell Tissue Res 1996;283:159–165.
41. Cassiman D, Libbrecht L, Desmet V, *et al.* Hepatic stellate cell/myofibroblast subpopulations in fibrotic human and rat livers. J Hepatol 2002;36:200–209.
42. Cassiman D, Denef C, Desmet VJ, *et al.* Human and rat hepatic stellate cells express neurotrophins and neurotrophin receptors. Hepatology 2001;33:148–158.
43. Li Y, Wang J, Asahina K. Mesothelial cells give rise to hepatic stellate cells and myofibroblasts via mesothelial-mesenchymal transition in liver injury. Proc Natl Acad Sci USA 2013;110:2324–2329.

Journal of Gastroenterology and Hepatology

JGHF

doi:10.1111/jgh.12376

HEPATOLOGY

Relationship between inosine triphosphate genotype and outcome of extended therapy in hepatitis C virus patients with a late viral response to pegylated-interferon and ribavirin

Hoang Hai,* Akihiro Tamori,* Masaru Enomoto,* Hiroyasu Morikawa,* Sawako Uchida-Kobayashi,* Hideki Fujii,* Atsushi Hagihara,* Etsushi Kawamura,* Le Thi Thanh Thuy,* Yasuhito Tanaka† and Norifumi Kawada*

*Department of Hepatology, Osaka City University Graduate School of Medicine, Osaka, and †Department of Virology and Liver Unit, Nagoya City University Graduate School of Medical Sciences, Nagoya, Japan

Key words
extended therapy, HCV, *ITPA* genotype, treatment outcome.

Accepted for publication 12 August 2013.

Correspondence
Dr Akihiro Tamori, Department of Hepatology, Osaka City University Graduate School of Medicine, 1-4-3, Asahi-machi, Abenoku, Osaka 545-8585, Japan. Email: atamori@med.osaka-cu.ac.jp

Conflict of interest: In the past year, Dr Akihiro Tamori has received research funding from MSD K.K. Dr Yasuhito Tanaka has consulted for MSD K.K and Chugai Pharmaceutical Co., Ltd., and has received research funding from MSD K.K and Chugai Pharmaceutical Co., Ltd. Dr Norifumi Kawada has consulted for MSD K.K and Chugai Pharmaceutical Co., Ltd., and has received research funding from MSD K.K and Chugai Pharmaceutical Co., Ltd. Other authors report no conflicts of interest.

The English in this document has been checked by at least two professional editors, both native speakers of English. For a certificate, please see http://www.textcheck.com/certificate/mXLRyV

Abstract

Background and Aim: It is not yet clear which factors are associated with the outcome of 72-week treatment with pegylated-interferon and ribavirin (RBV) in patients with chronic hepatitis C virus (HCV) infection.

Methods: In 66 patients with HCV genotype 1 who had a late viral response (LVR) to 72-week treatment of pegylated-interferon and RBV, we examined the factors that determined the outcome, including single nucleotide polymorphisms of interleukin-28B and inosine triphosphatase (*ITPA*) genes.

Results: Thirty seven of 66 (56%) patients with LVR achieved a sustained viral response (SVR). The mean age of these 37 SVR patients was 55, compared with 61 in 29 relapsed patients ($P = 0.009$). Twenty six of 54 (48%) patients with the CC genotype and 11 of 12 (92%) with the CA/AA genotype of *ITPA* rs1127354 achieved SVR ($P = 0.006$). The SVR rates were 79%, 40%, 60%, and 33% in patients with undetectable HCV RNA on weeks 16, 20, 24, and 28 or later, respectively ($P = 0.014$). Finally, serum RBV concentration at week 44 of treatment was significantly higher in the SVR group (2651 ng/mL) than in the relapse group (1989 ng/mL, $P = 0.002$). In contrast, the rate of the interleukin-28B genotype was not different between the groups. Multiple regression analysis showed that age < 60 years, *ITPA* CA/AA genotype, and serum RBV concentration were significant independent predictive factors for SVR.

Conclusions: Our findings elucidated the association of four factors, including *ITPA* genotype, with the outcome of 72-week treatment in LVR patients.

Introduction

Hepatitis C virus (HCV) infection continues to be a major cause of liver cirrhosis and hepatocellular carcinoma.[1] An estimated 120–130 million people worldwide are infected with HCV.[2] Sustained viral response (SVR), defined as undetectable serum HCV RNA levels 24 weeks after cessation of therapy, is the aim of treatment. Although the current treatment regimen of pegylated-interferon (PEG-IFN) combined with ribavirin (RBV) greatly improved SVR in patients with HCV genotypes 2 and 3, the outcomes in patients with HCV genotype 1 and high viral load (> 10^5 IU/mL) remain unsatisfactory, and SVR is attained in approximately 50% of cases.[3–8]

For HCV genotype 1, patients with rapid viral response, defined as undetectable serum HCV on week 4, achieve high rates of SVR up to 91% with combination therapy. Patients with early viral

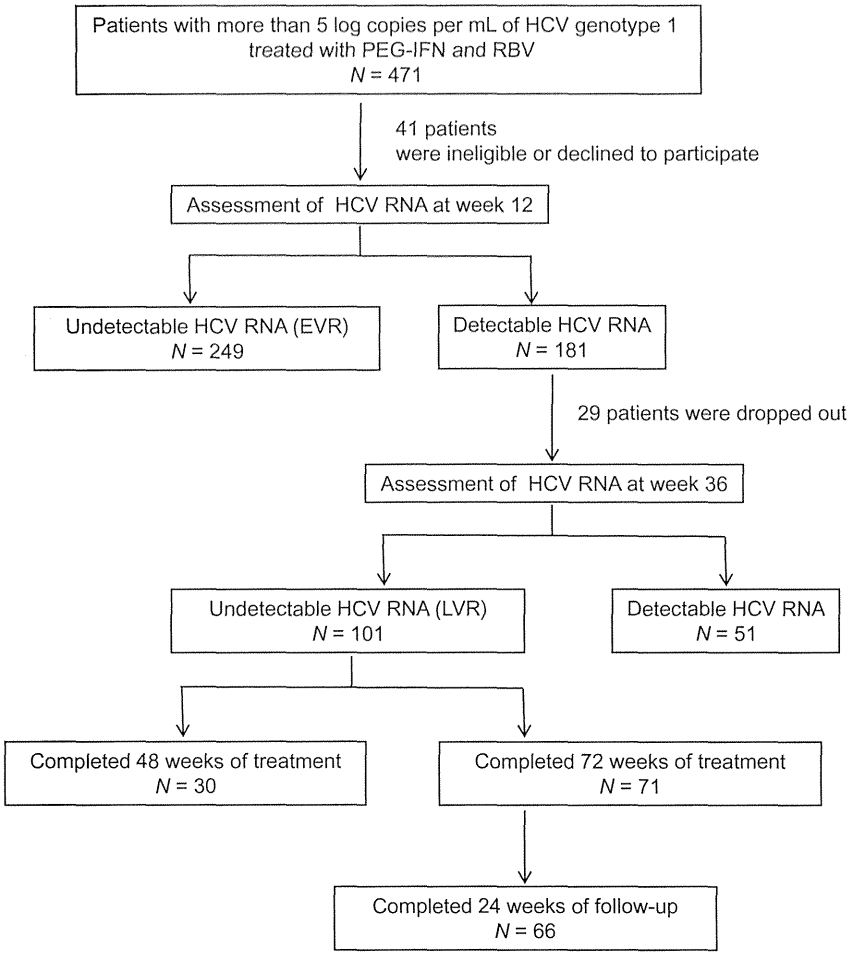

Figure 1 Flow of participants throughout the study. EVR, early viral response; HCV, hepatitis C virus; LVR, late viral response; PEG-IFN, pegylated-interferon; RBV, ribavirin.

response, defined as undetectable serum HCV on week 12, achieved SVR rates of 65–81%. However, patients with a late viral response (LVR), who remained positive for HCV RNA on week 12 after the start of treatment but became negative for HCV RNA during weeks 13–36 of treatment, showed a lower SVR rate of 14–44%.[4,9–19] Although extending therapy to 72 weeks has been reported to decrease relapse in such patients,[12–17,20,21] it remains unclear which patient with LVR can benefit from extended treatment.

Inosine triphosphatase (*ITPA*) single nucleotide polymorphism (SNP) rs1127354, causing ITPase deficiency, was found to be associated with protection from RBV-induced anemia and to decrease the need for RBV dose reduction, but not to be associated with clinical outcome.[22–25] The present study was performed to identify that factors, including interleukin-28B (*IL28B*) and *ITPA* genotype, associated with the outcome of extended 72-week treatment in patients with HCV genotype 1 who had LVR to PEG-IFN and RBV.

Methods

Patients. A total of 471 patients were recruited at Osaka City University Hospital between December 2004 and June 2012. The flow of patients through the trial is presented in Figure 1. Sixty-six patients with HCV genotype 1 who were treated with PEG-IFN alpha 2a (Pegasys; Chugai Pharmaceutical Co., Ltd, Tokyo, Japan) or 2b (Pegintron; MSD, Osaka, Japan) and RBV (Rebetol, MSD) combination therapy were enrolled in this study. All patients had a viral load of $> 10^5$ IU/mL according to COBAS Amplicor HCV Monitor test, version 2.0 (Roche Diagnostics, Branchburg, NJ, USA), or a viral load of > 5 log copies/mL as determined by COBAS TaqMan HCV test (Roche Diagnostics). HCV RNA levels were investigated before and every 4 weeks after the start of treatment. All patients gave written informed consent to participate in this study, in accordance with the ethical guidelines of the 1975 Declaration of Helsinki and according to the process approved by the ethical committee of Osaka City University, Graduate School of Medicine. Only the patients who completed 72-week combination therapy without discontinuation and in whom HCV RNA was detected on week 12 but not on weeks 13–36 were enrolled in this study.

Exclusion criteria included a history or evidence of a serious chronic or poorly controlled medical or psychiatric condition, infection with human immunodeficiency virus or hepatitis B virus, and receipt of systemic immunomodulatory or antineoplastic therapy within the previous 6 months. Pregnant or breastfeeding women and partners of pregnant women were also excluded.

The following factors were analyzed to determine whether they were related to the efficacy of combination therapy: patient age, gender, pretreatment biochemical parameters, such as neutrophil and platelet counts, hemoglobin concentration, levels of alanine transaminase, creatinine, HCV viral load, histopathological evaluation of hepatitis activity and hepatic fibrosis according to the METAVIR scoring system, total doses of PEG-IFN and RBV, and serum RBV concentration at week 44.

Treatment protocol. The initial dose of PEG-IFN alpha 2a was 180 μg per week, and that of PEG-IFN alpha 2b was 1.5 μg per kg body weight per week. The initial dose of RBV was 400, 600, 800, or 1000 mg/day for patients weighing < 40 kg, 40–60 kg, 60–80 kg, or > 80 kg, respectively.

RBV concentration. Serum RBV concentration was measured using an assay consisting of phenylboronic acid solid phase extraction, followed by HPLC at a commercial laboratory (SRL Inc., Osaka, Japan).[26] Briefly, the RBV concentrations in 200-μL samples were measured by validated HPLC with column switching. Serum samples deproteinized with perchloric acid were injected into the column, and RBV was detected by monitoring absorption of ultraviolet at 215 nm. The calibration curve was linear in the range of 50–20 000 ng/mL. A set of calibration standards at 0, 5, 10, 25, 50, 100, 250, 500, 1000, 2000, and 5000 mg/L RBV was prepared, extracted and analyzed with each series, together with internal quality controls at three levels.

SNP genotyping. We examined genetic polymorphisms of the *IL28B* and *ITPA* genes in patients who consented to genome analysis. Whole blood was collected from all patients and centrifuged to separate the buffy coat. Genomic DNA was extracted from the buffy coat using a QIAamp DNA Blood Midi Kit (Qiagen Sciences Inc, Germantown, MD, USA). Genetic polymorphisms of *IL28B* rs8099917 and rs12979860 and *ITPA* rs1127354 were genotyped by TaqMan SNP Genotyping Assay on the 7500 Fast Real-Time PCR System (Applied Biosystems, Foster City, CA, USA). All samples were also genotyped by direct sequencing to confirm the genotype. Exon 2 of the *ITPA* gene and flanking intronic regions were amplified by polymerase chain reaction (PCR) using the following primers: forward, 5′-CTTTAGG AGATGGGCAGCAG-3′; reverse, 5′-CACAGAAAGTCAGGTC ACAGG-3′.[27] PCR was carried out in a total volume of 15 μL with 1× Premix Ex Tag (Applied Biosystems), 300 nM of each primer, and 100 ng of genomic DNA. The PCR profile consisted of 94°C for 10 min, followed by 35 cycles of 94°C for 30 s, 63°C for 30 s, and 72°C for 1 min, with a final extension at 72°C for 7 min. PCR products were sequenced bidirectionally using a BigDye Terminator v3.1 Cycle Sequencing Kit and ABI 3130XL Genetic Analyzer (Applied Biosystems). Genotyping analysis was permitted by the ethical committee of our university (approval number 1871).

Statistical analysis. All data analyses were conducted using the JMP program, version 9.0 (SAS Institute, Cary, NC, USA). Individual characteristics between groups were evaluated by Wilcoxon's two-sample test for numerical variables, or Fisher's exact test for categorical variables. Variables exhibiting values of $P < 0.1$ on univariate analysis were subjected to stepwise multivariate logistic regression analysis. In the two-tailed test, $P < 0.05$ was taken to indicate statistical significance.

Table 1 Characteristics of HCV genotype 1 patients with late virologic response†

	Total (n = 66)
Age (years)	60 (21–77)
Gender (male/female)	43/23
HCV viral load (log copies/mL)	6.5 (5.1–7.7)
Body mass index (kg/m^2)	22.7 (16.5–28.0)
WBC (/μL)	4600 (2000–8600)
Hb (g/dL)	13.6 (10.9–17.3)
Platelet (× 10^4/μL)	17.1 (8.5–45.0)
ALT (IU/L)	54 (17–194)
Creatinine (mg/dL)	0.66 (0.36–1.16)
IL28B rs8099917 (TT/TG+GG)	45/21
IL28B rs12979860 (CC/CT+TT)	44/22
ITPA rs1127354 (CC/CA+AA)	54/12
Liver biopsy	
Activity grading (0/1/2/3/ND)	7/40/13/1/5
Fibrosis staging (1/2/3/4/ND)	38/15/8/0/5
PEG-IFNα2a/PEG-IFNα2b	12/54
Week when HCV RNA was undetectable (16 weeks/20 weeks/24 weeks/28 weeks or delayed)	24/20/10/12
RBV concentration at week 44 (ng/mL)	2467 (1006–4283)
Total dose of administered RBV (g/kg body weight)	5.07 (1.56–7.21)

†Continuous variables are medians (min-max).
ALT, alanine transaminase; Hb, hemoglobin; HCV, hepatitis C virus; *IL28B*, interleukin 28B gene; *ITPA*, inosine triphosphatase gene; ND, not done; PEG-IFN, pegylated-interferon; RBV, ribavirin; WBC, white blood cell.

Results

Patient profile and response rate. The characteristics of the overall 66 LVR patients, consisting of 43 men and 23 women, are shown in Table 1. The mean age of this cohort was 60 years. All of the patients who were infected with HCV genotype 1 with viral load > 5 log copies/mL, were treated with PEG-IFN/RBV for 72 weeks. HCV RNA was tested 24 weeks after completion of treatment when SVR and relapse were defined if HCV RNA was negative and positive, respectively. After 72 weeks of combination therapy, 37 (56%) patients achieved SVR, while the remaining 29 (44%) relapsed.

Direct sequencing and TaqMan SNP genotyping assay were used to genotype SNP *ITPA* rs1127354, and 100% of SNP results were concordant between both methods. Among the 66 LVR patients, 54 (82%) had the major CC genotype (wild-type), 10 (15%) were heterozygous for the CA genotype, and the remaining 2 (3%) had the minor AA genotype.

Association between clinical factors and SVR rate. Among the 17 factors screened by univariate analysis, four factors were associated with treatment response, that is, patient

Table 2 Comparison of the clinical characteristics of patients with SVR and those with relapse†

	SVR (n = 37)	Relapse (n = 29)	P-value
Age (years)	55 ± 7	61 ± 7	0.009*
Gender (male/female)	24/13	19/10	0.956
HCV viral load (log copies/mL)	6.6 ± 0.4	6.4 ± 0.5	0.195
Body mass index (kg/m^2)	22.6 ± 2.9	22.1 ± 2.5	0.438
WBC (/μL)	4748 ± 1235	4693 ± 1281	0.861
Hb (g/dL)	13.9 ± 1.3	13.9 ± 1.6	0.892
Platelets (× 10^4/μL)	18.2 ± 7.8	16.6 ± 4	0.698
ALT (IU/L)	63.8 ± 40.6	62.6 ± 37.9	0.861
Creatinine (mg/dL)	0.71 ± 0.19	0.67 ± 0.12	0.473
IL28B rs8099917 (TT/TG+GG)	25/12	20/9	0.904
IL28B rs12979860 (CC/CT+TT)	24/13	20/9	0.930
ITPA rs1127354 (CC/CA+AA)	26/11	28/1	0.006*
Liver biopsy			
Activity grading (0/1/2/3/ND)	3/24/6/1/3	4/16/7/0/2	0.563
Fibrosis staging (1/2/3/4/ND)	20/11/3/0/3	18/4/5/0/2	0.211
PEG-IFNα2a/PEG-IFNα2b	6/31	6/23	0.64
Week when HCV RNA was undetectable (16 weeks/20 weeks/24 weeks/28 weeks or delayed)	19/8/6/4	5/12/4/8	0.014*
RBV concentration at week 44 (ng/mL)	2651 ± 675	1989 ± 525	0.002*
Total dose of RBV administered (g/kg body weight)	5.08 ± 1.3	4.59 ± 1.11	0.059

*P < 0.05.

†Continuous variables are medians (min-max).

ALT, alanine transaminase; Hb, hemoglobin; HCV, hepatitis C virus; *IL28B*, interleukin 28B gene; *ITPA*, inosine triphosphatase gene; ND, not done; PEG-IFN, pegylated interferon; RBV, ribavirin; WBC, white blood cell.

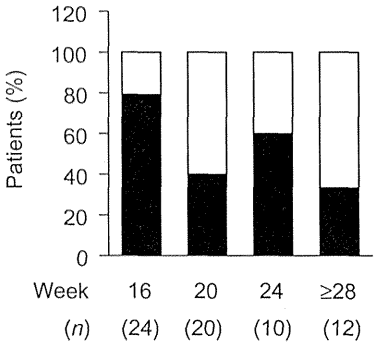

Figure 2 Effects of combination therapy in patients with genotype 1 according to the time at which HCV was undetectable (week). Earlier HCV RNA disappearance was significantly associated with treatment outcome (P = 0.014). SVR rates were 79% (19/24) in patients with undetectable HCV RNA at week 16, 40% (8/20) at week 20, 60% (6/10) at week 24, and 33% (4/12) at week 28 or delayed. HCV, hepatitis C virus; SVR, sustained viral response. (□) Relapse, (■) SVR.

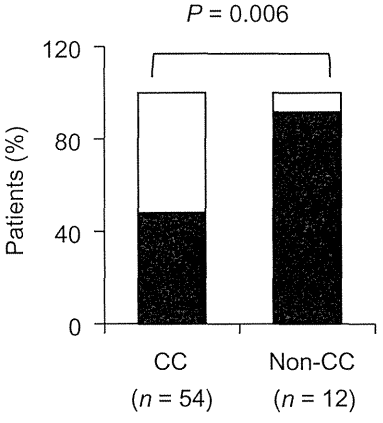

Figure 3 Effects of combination therapy in patients with genotype 1 according to *ITPA* SNP rs1127354 genotype. SVR (black bar) was achieved in 48% (26/54) of patients with the rs1127354 CC genotype, and in 92% (11/12) of those with a non-CC genotype at rs1127354. Patients with the rs1127354 CA/AA genotype were significantly more likely to be associated with SVR (P = 0.006). In the relapse group (white bar), the major CC allele occurred in 28/54 patients but the minor CC allele in only 1/12 patients. *ITPA*, inosine triphosphatase gene; SNP, single nucleotide polymorphism; SVR, sustained viral response. (□) Relapse, (■) SVR.

age, *ITPA* SNP rs1127354, time of undetectable HCV RNA, and RBV concentration (Table 2). The mean age of patients with SVR was significantly younger than that of patients with relapse (55 *vs* 61 years, respectively, P = 0.009). Eleven of 37 (30%) patients with SVR and 1 of 29 (3%) patients with relapse had the CA/AA genotype of *ITPA*, indicating a significant association between the CA/AA genotype and SVR (P = 0.006). In contrast, the proportion of the *IL28B* genotype was not different between patients with SVR and relapse. Earlier HCV RNA disappearance was significantly associated with treatment outcome (P = 0.014); SVR rate was 79% (19/24) in patients with undetectable HCV RNA on week 16, 40% (8/20) on week 20, 60% (6/10) on week 24, and 33% (4/12) on or after week 28 (Fig. 2). Finally, when RBV concentration in the peripheral blood was examined on week 44 of treatment, it was significantly higher in the SVR group (2651 ng/mL) than the relapse group (1989 ng/mL, P = 0.002).

Association between SNP ITPA rs1127354 and clinical factors. Twenty six of 54 (48%) patients with the CC genotype and 11 of 12 (92%) with the CA/AA genotype achieved SVR (Fig. 3), indicating a significant association between the CA/AA genotype and SVR (P = 0.006). The decline in hemoglobin concentration on week 12 from the baseline was 3.56 g/dL in patients with the CC genotype, compared with 2.16 g/dL in CA/AA patients (P = 0.0004, Fig. 4a).

Evaluation of the association between SNP rs1127354 and RBV concentration or total dose of administered RBV showed no significance (P = 0.27 and 0.65, respectively) (Fig. 4b,c).

Independent predictive factors of combination therapy for SVR. Factors exhibiting values of P < 0.1 on univariate analysis were age, *ITPA* genotype, week at which HCV

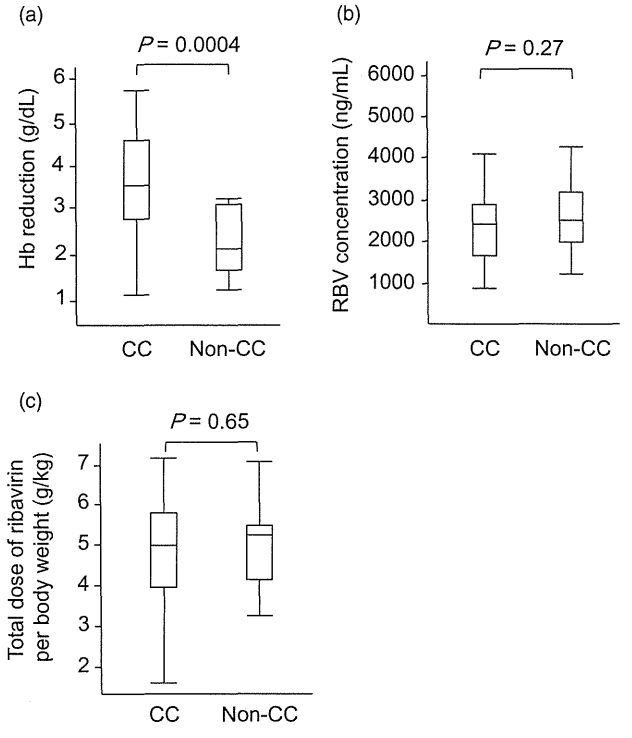

Figure 4 Association between *ITPA* polymorphism and clinical factors: hemoglobin reduction at week 12 (a), ribavirin concentration at week 44 (b), and total dose of administered ribavirin (mg/kg of body weight (c). Hb reduction in wild-type (CC) was significantly higher than those with heterozygous (CA) or homozygous (AA) rs1127354 (3.56 *vs* 2.16 g/dL, respectively, $P = 0.0004$). There were no significant associations between *ITPA* SNP rs1127354 and ribavirin concentration and total ribavirin dose administered ($P = 0.27$ and 0.65, respectively). *ITPA*, inosine triphosphatase gene; SNP, single nucleotide polymorphism.

RNA was undetectable, RBV concentration, and total dose of RBV administered. These factors were categorized below: (i) younger or older than 60 years, (ii) CC or non-CC genotype of *ITPA* SNP rs1127354, (iii) HCV RNA undetectable at < 24 weeks or ≥ 24 weeks, (iv) RBV concentration < 2500 ng/mL or ≥ 2500 ng/mL, and (v) total RBV dose of < 4.9 g/kg or ≥ 4.9 g/kg. Multiple regression analysis indicated that age, *ITPA* rs1127354, and RBV concentration were significant independent predictive factors for SVR ($P = 0.002$, 0.006, and 0.045, respectively Table 3).

Discussion

Previous studies have shown that extended 72-week combination therapy with PEG-IFN/RBV improves SVR rate,[14,15] while extended treatment is recommended only for HCV genotype 1 infection with LVR but not for general HCV patients.[13] However, Buti *et al.* showed that SVR rates were similar among LVR patients who received a standard dose of PEG-IFN alpha-2b and weight-based RBV for 48 or 72 weeks.[17] Although the overall SVR rate has been shown to improve in patients with LVR, it is necessary to determine which group of patients can benefit from extended therapy. The present study showed that age, timing of HCV RNA disappearance, serum RBV concentration, and *ITPA* SNP rs1127354 were related to the outcome of 72-week PEG-IFN/RBV therapy for patients with LVR.

Table 3 Multiple regression analysis

	Odds ratio (95% CI)	*P*-value
Age (≥ 60 years/< 60 years)	9.7 (1.8–82.6)	0.005*
ITPA rs1127354 (CA/AA *vs* CC)	15.8 (1.7–415)	0.012*
At week of undetectable HCV RNA (> 24 weeks/≤ 24 weeks)	1.1 (0.2–6.4)	0.897
Ribavirin concentration on week 44 (≥ 2500 ng/mL/< 2500 ng/mL)	12 (2.2–105.4)	0.003*
Total dose of ribavirin administered (≥ 4.9 g/kg/< 4.9 g/kg)	2 (0.4–9.7)	0.361

*$P < 0.05$.
HCV, hepatitis C virus; *ITPA*, inosine triphosphatase gene.

However, *IL28B* SNPs were not associated with the outcome of 72-week treatment in patients with LVR. *IL28B* SNP was originally reported as a host marker to predict null responders to 48-week treatment.[28] The patients enrolled in our study were late viral responders, but not null responders. Including only patients with a specific on-treatment viral response may reduce the influence of *IL28B* SNP on the outcome. Our results are consistent with those of Mangia *et al.*,[29] showing that *IL28B* genotyping had limited clinical utility in the arrangement of response-guided therapy for patients with genotype 1.

In contrast, 11 (92%) of 12 patients with CA or AA at *ITPA* SNP rs1127354 achieved SVR among 66 patients with LVR. Polymorphic variation in the *ITPA* gene causing ITPase deficiency leads to an elevated concentration of inosine triphosphate (ITP) in erythrocytes. Similarly, RBV-induced anemia is triggered by the accumulation of RBV active forms of triphosphate (RBV-TP) in erythrocytes. ITP competes with RBV-TP, thus protecting cells from the lytic effects of RBV-TP. Patients with the rs1127354 CA/AA genotype have a lower risk for a hemoglobin decline of > 3 g/dL.[22,30] In fact, we found that hemoglobin was significantly lower in patients with the CC genotype than in those with the CA/AA genotype during the initial 12 weeks of treatment (Fig. 4a). It has been reported that a cumulative reduction in RBV is more frequent in patients with the CC genotype than in patients who are non-CC. Additionally, *ITPA* SNP rs1127354 is one of the predictive factors for SVR.[31] However, other studies have shown that *ITPA* SNP is associated with RBV-induced anemia but not with treatment outcome in patients who undergo standard therapy.[22–25] In the 165 patients who underwent 48 weeks of therapy in our hospital, *ITPA* genotype was not related to outcomes of patients who underwent standard therapy (data not shown). In the present study, LVR patients were the subjects. We speculate that LVR patients have different clinical backgrounds, including genotype, related to outcome of PEG-IFN and RBV combination therapy. In a subset of patients with the favorable TT genotype of *IL28B* SNP rs8099917, rs1127354 SNP of *ITPA* seemed to be associated with the outcome of combination therapy.[32] This is the first study to demonstrate an association between *ITPA* SNP and SVR rate in LVR patients who underwent extended treatment.

It is unclear why the *ITPA* genotype was associated with outcomes of LVR patients who underwent extended treatment. It has been reported that expression of several genes before combination therapy is related to *ITPA* genotype.[30] One of these might play an important role in the response to elongated therapy. In the present study, seven of 10 patients with *ITPA* non-CC type showed > 2500 ng/mL RBV at week 44. In contrast, 19 of 41 patients with the *ITPA* CC type had > 2500 ng/mL RBV at week 44. Many patients with *ITPA* non-CC type had > 2500 ng/mL RBV at week 44.

We did not detect associations between *ITPA* variants and RBV concentrations at week 44 (Fig. 4b). RBV concentration is affected by both the dose administered and its clearance; the latter is regulated by renal function.[33] Serum creatinine level was within the normal range in the patients included in the present study, indicating that their renal function is sufficient to receive RBV adjusted by body weight. The RBV dose administered is dependent on body weight and is correlated with RBV-related adverse events, particularly anemia. Recently, it was reported that both *SLC28A2* rs11854484 genotype and *ITPA* genotype were related to RBV-related anemia. However, the factor associated with RBV concentration at weeks 4 and 8 was the *SLC28A2* rs11854484 genotype, but not the *ITPA* genotype.[34] In patients with LVR, RBV concentration and *ITPA* genotype were independently associated with the outcome of extended treatment (Table 3).

Our data suggest that serum RBV concentration at week 44 was significantly higher in patients with SVR than in those with relapse ($P = 0.002$). On the other hand, total dosage of RBV was not related to the outcome of extended therapy. In previously published data regarding 48-week therapy, both the RBV dose administered and the RBV concentration in peripheral blood were associated with the outcome of combination therapy with PEG-IFN and RBV.[35,36] Furusyo *et al.* reported that in both groups with < 60% and ≥ 60% of RBV assigned total dosage, the mean RBV concentration at 48 weeks in patients with SVR was > 1500 ng/mL and was significantly higher than in those with relapse, suggesting that RBV concentration was unaffected by the assigned total dosage.[37] In the present study, no association between RBV concentration on week 44 and the total dose of RBV administered was identified (data not shown).

Many novel interferon-free antiviral regimens for HCV are now under clinical investigation. Some of these include RBV in combination with one or two direct-acting antiviral agents.[38,39] RBV will remain a key drug for treatment of chronic HCV infection in the forthcoming era of oral combination antiviral therapy. Further studies are required to evaluate the significance of *ITPA* SNP as predictors of not only RBV-induced anemia but also of treatment outcome.

In conclusion, age, RBV concentration, timing of HCV RNA disappearance, and *ITPA* SNP rs1127354 were associated with a higher SVR rate in LVR patients given 72-week treatment. These predictive factors may allow more efficient extended treatment with PEG-IFN and RBV for patients with LVR.

Acknowledgments

We thank Ms. Yoko Yasuhara and Ms. Sanae Deguchi for their assistance in data/sample collection.

References

1 Shepard CW, Finelli L. Global epidemiology of hepatitis C virus infection. *Lancet Infect. Dis.* 2005; **5**: 558–67.
2 Global Burden of Hepatitis C Working Group. Global burden of disease (GBD) for hepatitis C. *J. Clin. Pharmacol.* 2004; **44**: 20–9.
3 Manns MP, McHutchison JG, Gordon SC *et al.* Peginterferon alfa-2b plus ribavirin compared with interferon alfa-2b plus ribavirin for initial treatment of chronic hepatitis C: a randomized trial. *Lancet* 2001; **358**: 958–65.
4 Fried MW, Shiffman ML, Reddy KR *et al.* Peginterferon alfa-2a plus ribavirin for chronic hepatitis C virus infection. *N. Engl. J. Med.* 2002; **347**: 975–82.
5 Hadziyannis S, Sette H Jr, Morgan TR *et al.* Peginterferon-alfa-2a plus ribavirin combination therapy in chronic hepatitis C: a randomized study of treatment duration and ribavirin dose. *Ann. Intern. Med.* 2004; **40**: 346–55.
6 Zeuzem S, Hultcrantz R, Bourliere M *et al.* Peginterferon alfa-2b plus ribavirin for treatment of chronic hepatitis C in previously untreated patients infected with HCV genotypes 2 or 3. *J. Hepatol.* 2004; **40**: 993–9.
7 Yamaguchi Y, Tamori A, Tanaka Y *et al.* Response-guided therapy for patients with chronic hepatitis who have high viral loads of hepatitis C virus genotype 2. *Hepatol. Res.* 2012; **42**: 549–57.
8 Zeuzem S. Heterogeneous virologic response rates to interferon-based therapy in patients with chronic hepatitis C: who responds less well? *Ann. Intern. Med.* 2004; **140**: 370–81.
9 Ferenci P, Fried MW, Shiffman ML *et al.* Predicting sustained virologic responses in chronic hepatitis C patients treated with peginterferon alfa-2a (40 KD)/ribavirin. *J. Hepatol.* 2005; **43**: 425–33.
10 Jensen DM, Morgan TR, Marcellin P *et al.* Early identification of HCV genotype 1 patients responding to 24 weeks peginterferon alpha-2a (40 kd)/ribavirin therapy. *Hepatology* 2006; **43**: 954–60.
11 Dienstag JL, McHutchison JG. American Gastroenterological Association medical position statement on the management of hepatitis C. *Gastroenterology* 2006; **130**: 225–30.
12 Ferenci P, Laferl H, Scherzer TM *et al.* Peginterferon alfa-2a/ribavirin for 48 or 72 weeks in hepatitis C genotypes 1 and 4 patients with slow virologic response. *Gastroenterology* 2010; **138**: 503–12.
13 Berg T, von Wagner M, Nasser S *et al.* Extended treatment duration for hepatitis C virus type 1: comparing 48 versus 72 weeks of peginterferon-alfa-2a plus ribavirin. *Gastroenterology* 2006; **130**: 1086–97.
14 Sanchez-Tapias JM, Diago M, Escartin P *et al.* Peginterferon-alfa2a plus ribavirin for 48 versus 72 weeks in patients with detectable hepatitis C virus RNA at week 4 of treatment. *Gastroenterology* 2006; **131**: 451–60.
15 Pearlman BL, Ehleben C, Saifee S. Treatment extension to 72 weeks of peginterferon and ribavirin in hepatitis C genotype 1-infected slow responders. *Hepatology* 2007; **46**: 1688–94.
16 Mangia A, Minerva N, Bacca D *et al.* Individualized treatment duration for hepatitis C genotype 1 patients: a randomized controlled trial. *Hepatology* 2008; **47**: 43–50.
17 Buti M, Lurie Y, Zakharova N *et al.* Randomized trial of peginterferon alfa-2b and ribavirin for 48 or 72 weeks in patients with HCV genotype 1 and slow virologic response. *Hepatology* 2010; **52**: 1201–7.
18 McHutchison JG, Lawitz EJ, Shiffman ML *et al.* Peginterferon alfa-2b or alfa-2a with ribavirin for treatment of hepatitis C infection. *N. Engl. J. Med.* 2009; **361**: 580–93.
19 Oze T, Hiramatsu N, Yakushijin T *et al.* Pegylated interferon alpha-2b (PEG-IFN **a**-2b) affects early virologic response

dose-dependently in patients with chronic hepatitis C genotype 1 during treatment with PEG-IFN **a**-2b plus ribavirin. *J. Viral Hepat.* 2009; **16**: 578–85.
20 Oze T, Hiramatsu N, Yakushijin T *et al.* The efficacy of extended treatment with pegylated interferon plus ribavirin in patients with HCV genotype 1 and slow virologic response in Japan. *J. Gastroenterol.* 2011; **46**: 944–52.
21 Di Martino V. Response-guided peg-interferon plus ribavirin treatment duration in chronic hepatitis C: meta-analyses of randomized, controlled trials and implications for the future. *Hepatology* 2011; **54**: 789–800.
22 Fellay J, Thompson AJ, Ge D *et al.* ITPA gene variants protect against anemia in patients treated for chronic hepatitis C. *Nature* 2010; **464**: 405–8.
23 Ochi H, Maekawa T, Abe H *et al.* ITPA polymorphism affects ribavirin-induced anemia and outcomes of therapy-A genome-wide study of Japanese HCV virus patients. *Gastroenterology* 2010; **139**: 1190–7.
24 Thompson AJ, Fellay J, Patel K *et al.* Variants in the ITPA gene protect against ribavirin-induced hemolytic anemia and decrease the need for ribavirin dose reduction. *Gastroenterology* 2010; **139**: 1181–9.
25 D'Avolio A, Ciancio A, Siccardi M *et al.* Inosine triphosphatase polymorphisms and ribavirin pharmacokinetics as determinants of ribavirin-associate anemia in patients receiving standard anti-HCV treatment. *Ther. Drug Monit.* 2012; **34**: 165–70.
26 Tsubota A, Horose Y, Izumi N *et al.* Pharmacokinetics of ribavirin in combined interferon-alpha 2b and ribavirin therapy for chronic hepatitis C virus infection. *Br. J. Clin. Pharmacol.* 2003; **55**: 360–7.
27 Bakker JA, Lindhout M, Habets DD, van den Wijngaard A, Paulussen AD, Bierau J. The effect of ITPA polymorphisms on the enzyme kinetic properties of human erythrocyte inosine triphosphatase toward its substrates ITP and 6-Thio-ITP. *Nucleosides Nucleotides Nucleic Acids* 2011; **30**: 839–49.
28 Tanaka Y, Nishida N, Sugiyama M *et al.* Genome-wide association of IL28B with response to pegylated interferon-alpha and ribavirin therapy for chronic hepatitis C. *Nat. Genet.* 2009; **41**: 1105–9.
29 Mangia A, Thompson AJ, Santoro R *et al.* Limited use of interleukin 28B in the setting of response-guided treatment with detailed on-treatment virological monitoring. *Hepatology* 2011; **54**: 772–80.
30 Birerdinc A, Estep M, Afendy A *et al.* Gene expression profiles associated with anemia and ITPA genotypes in patients with chronic hepatitis C (CH-C). *J. Viral Hepat.* 2012; **19**: 414–22.
31 Azakami T, Hayes CN, Sezaki H *et al.* Common genetic polymorphism of ITPA gene affects ribavirin-induced anemia and effect of peg-interferon plus ribavirin therapy. *J. Med. Virol.* 2011; **83**: 1048–57.
32 Kurosaki M, Tanaka Y, Tanaka K *et al.* Relationship between polymorphisms of the inosine triphosphatase gene and anemia or outcome after treatment with pegylated interferon and ribavirin. *Antivir. Ther.* 2011; **16**: 685–94.
33 Morello J, Rodríguez-Novoa S, Jiménez-Nácher I, Soriano V. Usefulness of monitoring ribavirin plasma concentrations to improve treatment response in patients with chronic hepatitis C. *J. Antimicrob. Chemother.* 2008; **62**: 1174–80.
34 Rau M, Stickel F, Russmann S *et al.* Impact of genetic SLC28 transporter and ITPA variants on ribavirin serum level, hemoglobin drop and therapeutic response in patients with HCV infection. *J. Hepatol.* 2013; **58**: 669–75.
35 Ogawa E, Furusyo N, Kajiwara E *et al.* An inadequate dose of ribavirin is related to virological relapse by chronic hepatitis C patients treated with pegylated interferon alpha-2b and ribavirin. *J. Infect. Chemother.* 2012; **18**: 689–97.
36 Kurosaki M, Hiramatsu N, Sakamoto M *et al.* Age and total ribavirin dose are independent predictors of relapse after interferon therapy in chronic hepatitis C revealed by data mining analysis. *Antivir. Ther.* 2012; **17**: 35–43.
37 Furusyo N, Murata M, Ogawa E *et al.* Ribavirin concentration in the later stages of 48 week pegylated interferon-alpha2b plus ribavirin therapy for chronic hepatitis C is useful for predicting virological response. *J. Antimicrob. Chemother.* 2011; **66**: 1127–39.
38 Gane EJ, Stedman CA, Hyland RH *et al.* Nucleotide polymerase inhibitor sofosbuvir plus ribavirin for hepatitis C. *N. Engl. J. Med.* 2013; **368**: 34–44.
39 Poordad F, Lawitz E, Kowdley KV *et al.* Exploratory study of oral combination antiviral therapy for hepatitis C. *N. Engl. J. Med.* 2013; **368**: 45–53.

INTERNAL MEDICINE

□ CASE REPORT □

A Complete Response Induced by 21-day Sorafenib Therapy in a Patient with Advanced Hepatocellular Carcinoma

Atsushi Hagihara, Yuga Teranishi, Etsushi Kawamura, Hideki Fujii, Shuji Iwai, Hiroyasu Morikawa, Masaru Enomoto, Akihiro Tamori and Norifumi Kawada

Abstract

The response rate and overall survival after sorafenib administration in patients with advanced hepatocellular carcinoma are unsatisfactory. We herein present the case of a 65-year-old man with multiple lung metastases of hepatocellular carcinoma. Because the patient had liver cirrhosis of Child-Pugh B accompanied by pancytopenia, sorafenib administration was initiated at a dose of 400 mg daily. Although he received sorafenib for only 21 days, the patient exhibited complete regression of the tumors. There was no clinical evidence of recurrence without the administration of anticancer treatment. It is unique that short-term sorafenib treatment achieved a complete response.

Key words: sorafenib, complete response, hepatocellular carcinoma

(Intern Med 52: 1589-1592, 2013)
(DOI: 10.2169/internalmedicine.52.9340)

Introduction

Hepatocellular carcinoma (HCC) is one of the most common cancers worldwide (1). Resection and local ablation therapy, including radiofrequency ablation and percutaneous ethanol injection (PEI), are curative treatments for HCC (2-4). Transcatheter arterial chemoembolization (TACE) or transcatheter arterial embolization (TAE) are recommended as the first-line non-curative therapies for patients with large or multifocal unresectable HCC without vascular invasion or extrahepatic spread (4). However, the majority of patients develop recurrence or metastasis following these treatments. The prognosis of patients with advanced HCC remains poor. In addition, liver transplantation is not recommended for such patients due to the high risk of recurrence and poor outcome. Chemotherapy is recognized to be a palliative treatment for advanced HCC. Sorafenib, an oral multikinase inhibitor that targets Raf kinase and receptor tyrosine kinases (5), was found to prolong the overall survival and time to progression with manageable toxicity compared to a placebo in two phase III trials (6, 7). Therefore, sorafenib is now recommended as the first-line option in patients with a preserved liver function in whom resection, transplantation, local ablation therapy or TACE (TAE) are not effective. However, systemic chemotherapy is associated with unsatisfactory results in terms of response and survival in patients with advanced HCC. We herein report the case of a patient with multiple metastases of HCC that regressed following short-term treatment with sorafenib.

Case Report

The patient was diagnosed with chronic hepatitis C in 1988 when he was 43 years of age. In August 2001, at 56 years of age, a tumor in segment 3 of the patient's liver displayed the typical computed angiographic pattern of HCC, and TACE was performed. Subsequently, recurrence of HCC was observed, and the patient underwent PEI four times and TACE 10 times. In June 2010, computed tomography (CT) revealed invasion of the cancer into the inferior vena cava (IVC), and thus TAI with miriplatin hydrate (Dainippon Sumitomo Pharma Co., Ltd.) was administered. The cancer persisted, and the patient received particle beam radiation

Department of Hepatology, Osaka City University Hospital, Japan
Received for publication November 14, 2012; Accepted for publication March 7, 2013
Correspondence to Dr. Norifumi Kawada, kawadanori@med.osaka-cu.ac.jp

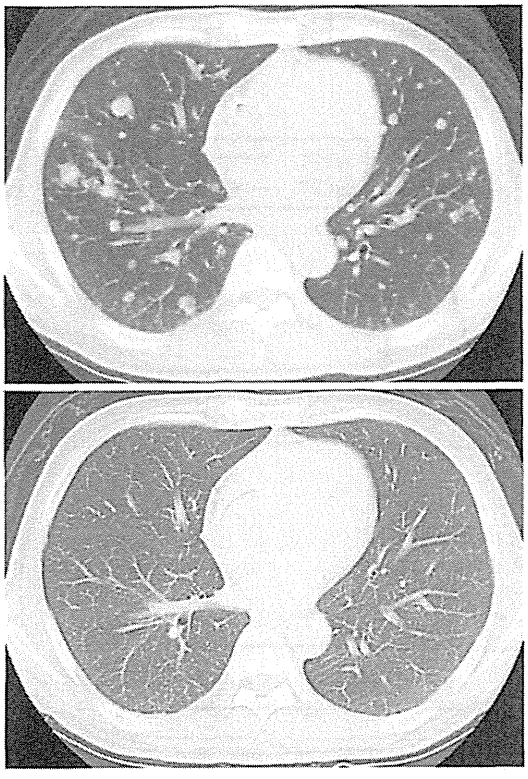

Figure 1. **Changes in the chest computed tomography (CT) findings. Upper chest CT showed multiple metastases in the lungs before the initiation of sorafenib administration. Lower chest CT revealed that metastasis was no longer present in the lungs following treatment.**

therapy for the cancer invading the IVC. In November 2010, multiple recurrence of HCC was observed in the liver and lungs. Because the patient had liver cirrhosis of Child-Pugh B accompanied by pancytopenia, we did not initiate sorafenib treatment and considered that controlling the HCC in the liver first would be better for the patient's prognosis. TACE was performed in December 2010 for recurrence of the HCC in the liver. In February 2011, when the patient was 65 years of age, CT revealed that the multiple metastases in the lungs would determine the patient's prognosis (the upper side of Fig. 1). On admission, laboratory examinations revealed the following values: aspartate aminotransferase (AST), 57 IU/L; alanine aminotransferase (ALT), 44 IU/L; bilirubin, 0.5 mg/dL; albumin, 2.8 g/dL; and prothrombin international normalized ratio (PT-INR), 1.18. The patient had severe ascites uncontrolled by furosemide treatment at a high dose (more than 80 mg/day), and no coma (Child-Pugh class B) was observed. Due to a low platelet count (36,000/μL), sorafenib administration was initiated at a dose of 400 mg daily on March, 2011. However, the sorafenib administration was discontinued on day 21 because the patient's general condition deteriorated, namely, the severe ascites worsened, a grade I hepatic coma appeared and the performance status (PS) was 3 immediately after starting the therapy. The patient was sent to a hospice to receive palliative care on March, 2011. Two months after the discontinuation of sorafenib therapy, the PS improved, and the patient was discharged from the hospice. The levels of alpha-fetoprotein (AFP) and des-gamma-carboxy prothrombin (DCP) at the start of sorafenib treatment were 55,607 ng/mL and 11,302 mAU/mL, respectively. After five months of treatment, these levels decreased to 5 ng/mL and 23 mAU/mL, respectively (Fig. 2). CT revealed that lung metastasis was no longer present (the lower side of Fig. 1). The administration of sorafenib was not started again due to the patient's poor liver function. In April 2012, 13 months after treatment, the patient died of acute myocardial infarction, and there was no clinical evidence of intra- or extrahepatic recurrence without any anticancer treatment.

Discussion

This case is a rare case of a complete remission following treatment with sorafenib in a patient with advanced HCC confirmed on the basis of imaging and the levels of tumor markers. Sorafenib has become the standard treatment option in patients in whom resection, transplantation, local ablation therapy and TACE cannot be performed. However, systemic chemotherapy with sorafenib is thought to be unsatisfactory in terms of response and survival in advanced HCC patients. Sorafenib therapy did not achieve a complete response in 299 patients in the Sorafenib Hepatocellular Carcinoma Assessment Randomized Protocol (SHARP) study or 150 patients in the Asian Pacific study; the partial response rates were 2.0% and 3.3%, respectively (6, 7). Only a few studies have reported a complete response in HCC patients receiving sorafenib treatment (8-16). We listed these in order of the time to cessation (Table). According to reports of a complete response in HCC patients receiving sorafenib treatment, the duration of sorafenib administration ranged from a minimum of four to 18 months. Our case is unique because the patient was treated with sorafenib for only 21 days. Our patient achieved a complete response within three months. We were unable to determine the exact time to the complete response because the patient was sent to a hospice to receive palliative care without undergoing an evaluation of the effect of sorafenib.

The HCC observed in this patient may have regressed spontaneously. Spontaneous regression is defined by Everson and Cole as involution of a malignant tumor without the application of a specific therapy (17, 18). Spontaneous regression of malignant tumors is estimated to occur in one out of 60,000-100,000 patients. Half of such patients have renal cell carcinoma, neuroblastoma or malignant melanoma, and spontaneous regression of HCC is extremely rare (19).

Sorafenib is a multikinase inhibitor that targets Raf kinase, vascular endothelial growth factor (VEGF), platelet-derived growth factor (PDGF), Fms-like tyrosine kinase 3 (Flt-3) and c-Kit receptor tyrosine kinase. It is metabolized by CYP3A4, CYP2B6, CYP2C9, CYP2C8, UGT1A1, UGT1A9 and so on (20). The sensitivity of the response to molecular target drugs is usually correlated with particular